Downloaded from rsta.royalsocietypublishing.org

PHILOSOPHICAL TRANSACTIONS OF THE ROYAL SOCIETY A MATHEMATICAL, PHYSICAL & ENGINEERING SCIENCES

Slow flow of granular aggregates: the deformation of sediments beneath glaciers

G. S. Boulton and K. E. Dobbie

Phil. Trans. R. Soc. Lond. A 1998 **356**, 2713-2745
doi: 10.1098/rsta.1998.0294

Email alerting service

Receive free email alerts when new articles cite this article - sign up in the box at the top right-hand corner of the article or click **here**

To subscribe to *Phil. Trans. R. Soc. Lond. A* go to: **http://rsta.royalsocietypublishing.org/subscriptions**

This journal is © 1998 The Royal Society

Downloaded from rsta.royalsocietypublishing.org

THE ROYAL SOCIETY

Slow flow of granular aggregates: the deformation of sediments beneath glaciers

By G. S. Boulton and K. E. Dobbie

Department of Geology and Geophysics, University of Edinburgh, Grant Institute, King's Buildings, West Mains Road, Edinburgh EH9 3JW, UK

Shear deformation of sediments is widespread beneath glaciers. Sediment rheology and the structure of the subglacial drainage system control the deformational behaviour of sediments and the way in which they play a role in determining the dynamics of glaciers, the magnitude of subglacial erosion, the nature of till deposition and many geotechnical properties of glacial sediments which are of concern to engineers. It is suggested that a power law relating shear strain rate, shear stress and effective stress is the most useful general description of their continuum behaviour. Evidence is reviewed from laboratory and field experiments, from the structural properties of tills and from the large-scale patterns of till deposition by former ice sheets to suggest the principal modes of rheological behaviour for tills of different granulometries and to speculate on the interparticle processes which determine them.

Keywords: till rheology; dilatant shear flow; rate-dependent flow; stick-slip; granulometry

1. Introduction: the glaciological and geological context

A glacier is a gravity flow of ice, metamorphosed from and driven by accumulation of snow high in its source region, and which flows to low elevations, where it is progressively destroyed by melting. Glaciers range in size from small channelled flows in mountain valleys to large continent-scale domes, such as the Antarctic ice sheet, several kilometres in thickness and several thousand kilometres in width. Experimentally determined flow rules for polycrystalline ice, which show a nonlinear creep response to stress (Glen 1955), have been successfully used to explain the gross distribution of mass and flow in glaciers. Early analyses invariably assumed that the glacier had a rigid rock bed, and that the flow response to atmospheric forcing was entirely determined by the rheological properties of ice (e.g. Nye 1957; Patterson 1981).

It was shown by Boulton & Jones (1979), however, that water-saturated, unlithified, granular sediments underlying a glacier underwent shear deformation in response to the gravity drive and that this process could account for a large part of the glacier's movement. As many modern glaciers flow over soft sediment beds and as the beds which underlay the ice sheets which covered much of Eurasia and North America as little as 15 000 years ago were composed of soft sediment, Boulton & Jones also suggested that the movement of many past and present glaciers could be a product of the coupled flow of ice and its deforming bed. Such two-layer flows have now been shown to occur in the Antarctic ice sheet (Alley *et al*. 1986; Kamb 1991) and many smaller glaciers (Blake & Clarke 1992; Humphrey *et al*. 1993; Iversen *et al*. 1995).

© 1998 The Royal Society
TEX Paper

Downloaded from rsta.royalsocietypublishing.org

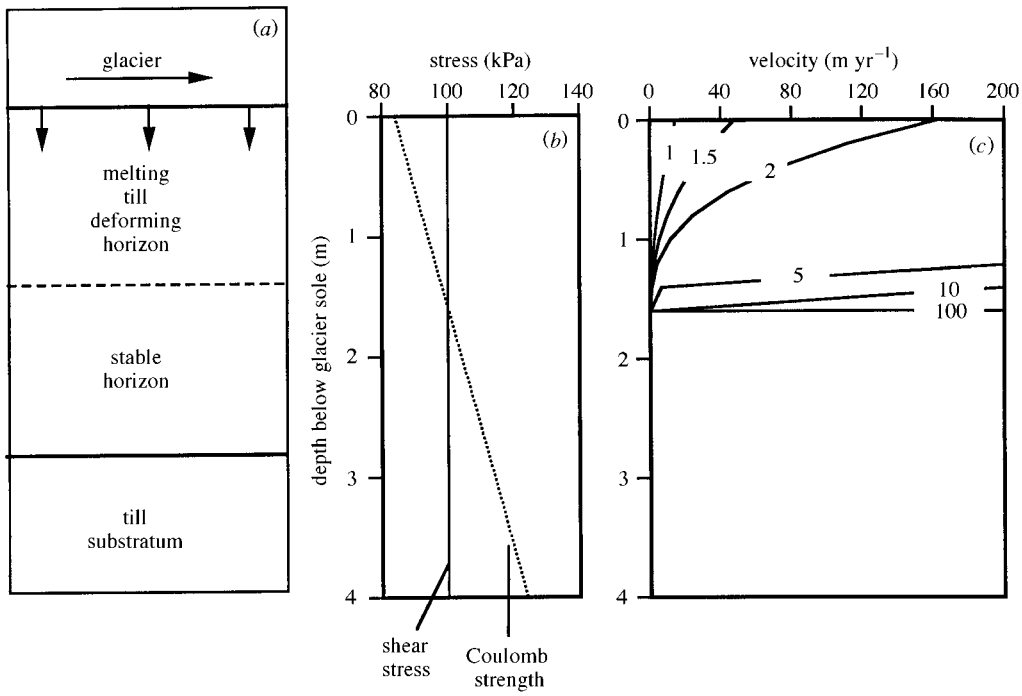

Figure 1. The setting for till deformation beneath glaciers. (*a*) A melting glacier moving over an unlithified sediment, the upper part or the whole of which may deform, overlying a rigid substratum which may be of greater or smaller permeability than the overlying sediment. (*b*) If glacier–bed coupling is strong, the glacially imposed shear stress will be constant with depth, but sediment strength will increase. Deformation will not occur below the depth where strength exceeds stress. (*c*) The strain response to the situation in (*b*) of sediments with different values of n in the flow law in equation (2.5).

Glaciated areas tend to have a more or less continuous cover of *till*, a sediment dominantly deposited at the base of a glacier, comprising a poorly sorted assemblage of granular materials, ranging from boulders to clays, derived by erosion of the substratum over which the glacier has flowed. The constituent rock and mineral grains may have been produced by crushing and grinding of hard rocks or deformation and mixing of particulate materials derived from pre-existing soft sediments. The formerly glaciated surfaces of Eurasia and North America have a widespread cover of till, typically between 2 m and 20 m in thickness. Clayton (1999) has calculated an average thickness of glacial sediment within the area of the last glaciation in Britain, of which about half is till of about 20 m, reduced by post-glacial erosion from about 27 m. It has been suggested (Boulton 1987; Alley 1991; Hart 1995) that the majority of tills deposited in the lowland areas of Eurasia and North America by ice sheet expansion during the Pleistocene were produced by deformation and mixing of pre-existing soft sediments as a consequence of subglacial shear deformation.

These issues are not only important in understanding the Earth's environmental history but have considerable practical implications for the construction industry in view of the severe engineering problems frequently produced by tills as a consequence of their mode of deposition (e.g. Trenter *et al*. 1997).

Downloaded from rsta.royalsocietypublishing.org

2. Implications of the choice of subglacial sediment rheology

Figure 1*a* shows the typical setting of a till bed beneath a glacier. Most glaciers melt at their base, and in the terminal zone at least, surface water can locally recharge the bed in summer through crevasses and moulins which penetrate to the bed. Otherwise, the glacier itself is assumed to be an aquiclude. Most tills are relatively impermeable and many lie on a more permeable substratum, for even ancient Shield rocks tend to be highly fractured and can have relatively high permeabilities (Wladis *et al.* 1997). Meltwater therefore tends to flow through the till into the underlying stratum, although, as this is unlikely to be an adequate drain for all the melt, channels occur at the ice–bed interface to drain the excess melt, and thereby determine the overall intergranular drainage pathways and the distribution of water pressure potentials. We assume that if there is strong coupling between the glacier and its bed, the shear stress imposed by the moving glacier (τ_b) will not decay with depth (figure 1*b*). Till strength will, however, increase with depth as a consequence of increasing effective pressure (p_e), which, in the absence of groundwater flow, will increase with depth as

$$\frac{\delta p_\mathrm{e}}{\delta z} = (1-n)(\rho_\mathrm{s}-\rho_\mathrm{w})g, \tag{2.1}$$

where n is the void ratio, ρ_s is the sediment grain density, ρ_w is the water density, and g is the acceleration due to gravity. A typical vertical effective pressure gradient is about $10\,\mathrm{kPa\,m^{-1}}$, although this can be much enhanced if downward meltwater flow through the till (figure 1*a*) produces a large negative vertical potential gradient ($\delta\psi/\delta z$), such that

$$\frac{\delta p_\mathrm{e}}{\delta z} = [(1-n)(\rho_\mathrm{s}-\rho_\mathrm{w})g] - \left(\frac{\delta\psi}{\delta z}\right) \tag{2.2}$$

(Boulton & Dobbie 1993). If the Coulomb yield stress (τ_C) of the till is

$$\tau_\mathrm{C} = p_\mathrm{e}\tan\phi \tag{2.3}$$

ignoring any strength component from cohesion, figure 1*b* shows how the overstress ratio in the till ($\tau_\mathrm{b}/\tau_\mathrm{C}$) will increase with depth. Once Coulomb failure has occurred, it has been suggested (Taylor 1942; Litkouhi & Poskitt 1980; Iverson 1985) that the most useful general flow rule relating strain rate ($\dot{\varepsilon}$) and excess stress ($\tau-\tau_\mathrm{C}$) is a power law of the form,

$$\dot{\varepsilon} = A(\tau-\tau_\mathrm{C})^n, \tag{2.4}$$

where A and n are constants. Boulton & Hindmarsh (1987) suggested that measured till behaviour beneath a glacier in Iceland could be approximated by a Bingham fluid or nonlinearly viscous model to produce a flow rule relating shear strain rate ($\dot{\varepsilon}$) in a deforming mass to effective pressure (p_e) and shear stress. For the Bingham model,

$$\dot{\varepsilon} = A\frac{(\tau-\tau_\mathrm{C})^n}{p_\mathrm{e}^m}. \tag{2.5}$$

Figure 2*a* shows the range of possible behaviour described by such a relationship. If we assume a finite yield stress for the sediment, a highly nonlinear strain rate response to stress (n very large) approximates to perfectly plastic or Coulomb behaviour, with linear viscoplastic behaviour as n approaches 1. The geometry of strain in a subglacial

Downloaded from rsta.royalsocietypublishing.org

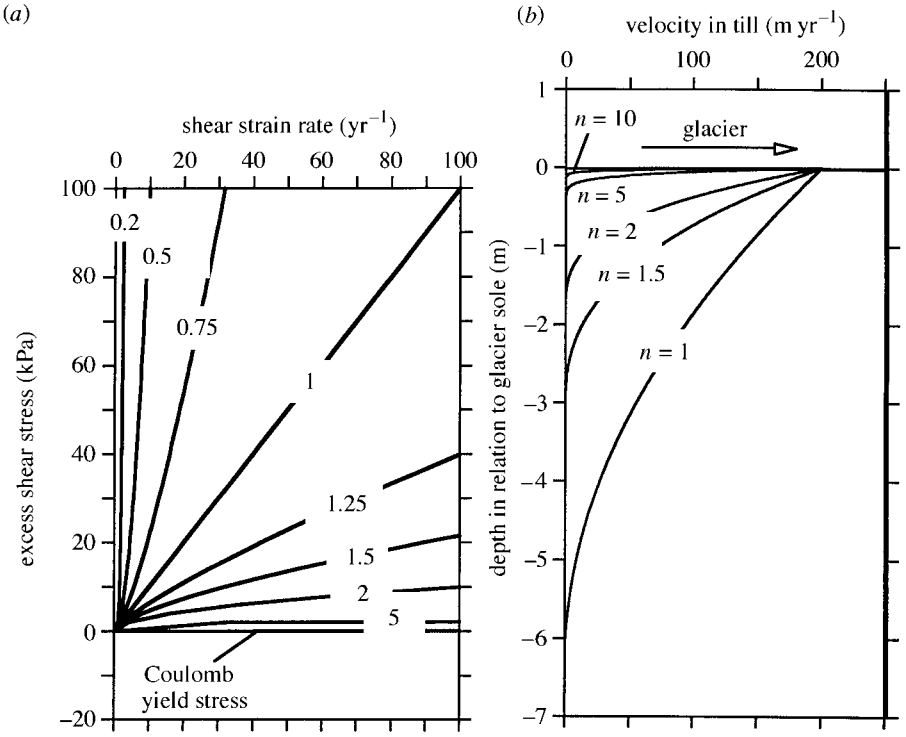

Figure 2. (*a*) A rheological model for soils in which the soil behaves in a viscous fashion at stresses above the Coulomb yield strength. (*b*) Beneath a glacier in steady state, system velocity is limited by mass balance. If all glacier movement is provided by bed deformation, sediments with low-n values will need to deform to greater depth to yield the requisite velocity. This implies that low-n sediments will tend to be eroded to greater depth and form greater thicknesses of till than high-n sediments.

bed with the distribution of safety factors shown in figure 1*b* is illustrated in figure 1*c* for the rheological behaviours shown in figure 2*a*.

The operational function of a deforming bed can be illustrated by the case where ice–bed coupling is very strong (no sliding at the interface) and where we assume that the ice is stiff compared to the bed, and thus that all forward movement of the glacier takes place as a consequence of bed deformation. In a steady state, the 'function' of glacier movement at any point is to discharge the integrated flux of accumulation which occurs up-glacier of that point. Figure 2*b* shows the velocity distributions required in tills with different values of n in equation (2.1) in order to produce a velocity of 200 m a^{-1} at the ice–bed interface for a constant shear stress (the range of shear stress at the base of a glacier is small, typically 50–150 kPa, such that steady-state glacier flow can be satisfactorily modelled by assuming a constant shear stress (e.g. Nye 1952)).

We therefore suggest that where subglacial deformation occurs, system behaviour is determined by one of two broad classes of rheological behaviour.

Class A *Behaviour approximately that of a perfectly-plastic Coulomb solid or Bingham fluid with large n* (*figure 2a, b, n* > 10)

Downloaded from rsta.royalsocietypublishing.org

In this case, if the shear stress at the base of the glacier attains the Coulomb yield stress of the subglacial sediment, strain occurs at whatever rate is required in the system without any change in stress. If the yield stress is low, and if the bed is entirely covered by sediment, its yield stress (τ_C) will control the maximum gravitational shear stress which can be generated in the ice sheet (τ_b) such that

$$\tau_b = \tau_C = \rho_i g h \sin \alpha, \tag{2.6}$$

where ρ_i is the density of ice, g is the acceleration due to gravity, h is the ice thickness and α is the surface slope. Such behaviour was analysed by Boulton & Jones (1979). The bed plays a binary role in ice sheet dynamics. If the conditions for Coulomb failure are met, most deformation is concentrated at the bed in a very thin layer, equivalent to sliding, and very little flow will occur in the ice which will be transported as a plug above the deforming bed. The rate of movement of the glacier and of flow in the bed will adjust to that required to discharge the climatically determined mass balance flux in the glacier. If Coulomb failure does not occur, the bed will be rigid and all flow will take place in the ice.

Class B *Behaviour that of a viscous or Bingham fluid with small n* ($n < 10$)

In this case, there will be a significant variation in strain rate for the range stresses, or the stresses in excess of yield stress, typically found at the base of a glacier. Bed deformation will not show the extreme sensitivity of class A, where there will either be no deformation or deformation at whatever rate is required to maintain the overlying ice flux, but will occur at whatever rate is determined by effective pressure and shear stress (equations (2.4) and (2.5)). Flow will tend to be partitioned between the ice and the deforming bed.

These two modes of behaviour are at the centre of current debate and have very different implications for glacial geology, geotechnical engineering and glaciology.

Implications for glacial geology If, as has been suggested (Boulton 1987; Alley 1991; Hart 1995), it is true that most tills in lowland areas were produced and emplaced by bed deformation, the deformation process is of central importance in glacial geology. For a glacier flowing over an approximately planar bed and near to a steady state, the accumulation area is generally a zone of accelerating flow and the ablation area one of decelerating flow. If there is strong coupling between the glacier and a deforming bed such that a large proportion of the motion of the glacier is accounted for by deformation of the bed, sediment deformation will produce erosion in the inner accelerating zone and deposition in the outer decelerating zone (figure 3; see also Boulton 1996). The rates of erosion and deposition will be low for class A behaviour and high for class B behaviour. Class A behaviour will tend to produce thin tills and class B thick tills.

Implications for geotechnical engineering Glacial tills pose severe problems for civil engineering construction because of the strong spatial variations in density shown by tills of similar granulometry and highly variable sensitivities to rapid loading. It is important to develop usable guides for site investigation which indicate how till distribution and density might vary. Class A behaviour is likely to lead to thin tills overlying relatively heavily consolidated sediments. Class B behaviour will produce thicker tills which are consolidated relatively lightly.

Downloaded from rsta.royalsocietypublishing.org

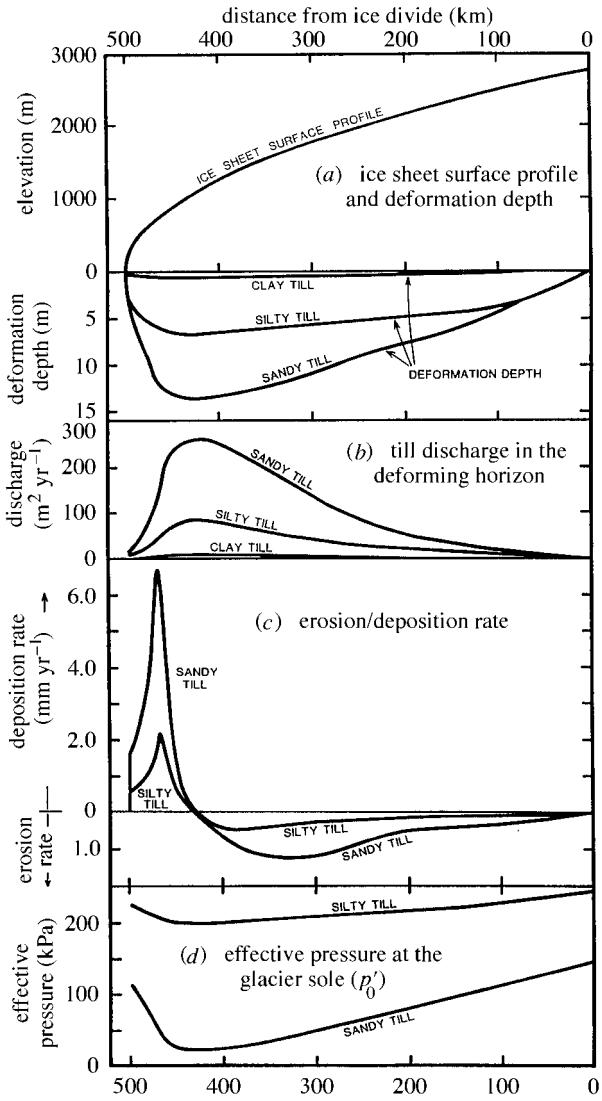

Figure 3. Large-scale consequences of different till rheologies beneath an ice sheet for a clay till with very large n, a sandy till with a very low n, and a silty till with an intermediate n value (Boulton 1996). (*a*) Depth to which till would deform. (*b*) Discharge of till in the deforming layer. (*c*) The rate of erosion in the up-glacier zone of accelerating flow and deposition in the terminal decelerating zone. (*d*) Required effective pressure at the glacier sole. It is assumed that glacier flow takes place exclusively by deformation in the bed, and that ice sheet profile and mass balance are fixed. It ignores coupling between ice sheet and bed.

Implications for ice sheet dynamics Many modern and Pleistocene glaciers are characterized by extensive zones of basal melting (Patterson 1994). If the efficiency by which drainage occurs at the base of the glacier is high (figure 4), meltwater will escape readily under relatively low potential gradients, water pressures will be low, effective pressures will be high, the strength of basal sediments will be high and movement be dominated by flow within the ice. If drainage is relatively

Downloaded from rsta.royalsocietypublishing.org

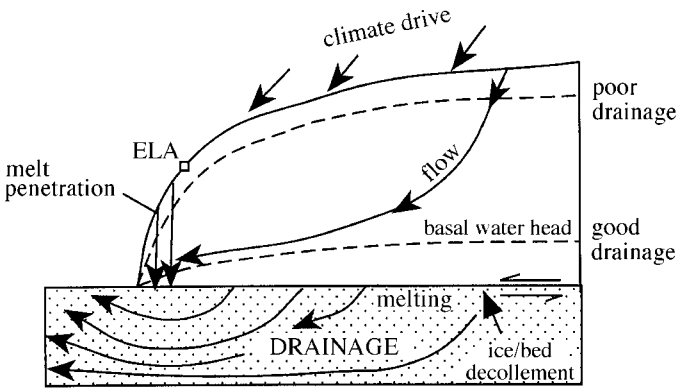

Figure 4. The role of subglacial drainage in determining properties of the setting in which subglacial sediment deformation occurs. Good drainage draws down water pressures, tends to inhibit deformation and any instability which arises from it, ensuring that ice processes are primarily responsible for flow in the system. Poor drainage, produces the opposite result, concentrates flow in any deformable sediments and produces complex glacier–bed coupling which may tend to instability. ELA refers to the equilibrium line altitude, where winter snow accumulation is balanced by summer melting.

inefficient, water pressures will be high, effective pressures will be low and sediment deformation (or slip at the ice–bed interface if ice–bed coupling is poor) will tend to play a major role in governing ice sheet movement. The shear stress at the base of a glacier (τ_b) tends to lie within a limited range, and can be regarded as approximately constant.

For class A behaviour, a critical effective pressure $(p_e)_{crit}$ can be defined from (2.3), given by

$$(p_e)_{crit} = (\tau_C)/\tan\phi, \tag{2.7}$$

which determines one of two possible dynamic states. If the effective pressure is larger than the critical value, there will be no deformation of the bed and forward movement will take place by flow in the ice and by conventional sliding mechanisms. There will be no coupling between bed and ice rheology. If the effective pressure is equal to or less than $(p_e)_{crit}$, failure will occur in a thin layer immediately beneath the glacier sole, which is equivalent to sliding, at whatever rate is required by the mass balance flux of the glacier. Stress is not rate dependent in a perfectly plastic or Coulomb flow. We therefore assume that the residual strength of the till will provide a bound for the minimum basal shear stress and thus determine a minimum slope profile for the glacier (equation (2.6)). Coupled, dynamic interaction between the bed and the glacier will largely be through drainage. The efficiency of subglacial drainage will determine the basal water pressure regime which, in turn, will determine whether effective pressures will be above or below $(p_e)_{crit}$ and therefore which mode of flow will occur (figure 4). Basal friction will vary according to the effective pressure at the glacier bed, which will influence the melt rate and thereby feed back to basal water pressure.

For class B behaviour, the precise values of effective pressure and shear stress, determined largely by drainage through the system, will determine the rate of shear deformation. Thus, there is continuous coupling between rheology and drainage

Downloaded from rsta.royalsocietypublishing.org

between glacier and bed mediated by the drainage system, rather than a mere bi-modal interaction.

3. The search for till rheology

The above implications of different rheological behaviours indicate the importance of understanding and characterizing them. We suggest that equations (2.4) and (2.5) provide a good general framework for empirical continuum descriptions of till rheology, the key issue being the values of the exponents which determine which class of behaviour, A or B, best describes the behaviour of till in general. Boulton & Hindmarsh (1987) used data from field experiments (Boulton & Jones 1979) from a subglacial setting similar to that shown in figure 1*a* beneath an Icelandic glacier, to define a Bingham rheology for a till such that

$$\dot{\varepsilon} = 7.62\left(\frac{p_e}{10^5}\right)^{-1.25}\left(\frac{\tau_b - \tau_C}{10^5}\right)^{-0.625}. \tag{3.1}$$

They used the same data to produce a model of nonlinearly viscous behaviour:

$$\dot{\varepsilon} = 3.99\left(\frac{p_e}{10^5}\right)^{-1.8}\left(\frac{\tau_b}{10^5}\right)^{-1.3}, \tag{3.2}$$

where stress and pressure are in Pa and strain rates in a^{-1}. In this case, the till appears to show class A behaviour.

It is important to distinguish, however, between an *intrinsic material property* of a till, governed by interparticle interactions and which one might measure in a laboratory, and its role as part of a complex natural *system*, which conditions its *behaviour* as measured in field experiments.

(*a*) *Intrinsic properties*

Mineralogy and granulometry are key determinants of intrinsic till properties. Figure 5 shows granulometric distributions in tills from three different areas, a sandy bouldery till derived from the primary erosion of igneous bedrock, and characteristic of the granulometry of tills found on the old shield areas which underlie the central zones of the Pleistocene ice sheets in Europe and North America, and silty and clay-rich tills derived from pre-existing sediments which surround the shields. The wide range of grain sizes which characterize these tills permits them to compact to high solid volume fractions, greater than 0.7–0.75, compared with maximum values of 0.65 achieved by close packing of equidimensional spheres. The proportion of different size fractions in a till, particularly the contrast between the clay and silt/sand fractions with their different mineralogies is clearly important in determining behaviour. Georgiannou *et al*. (1990) showed that the dilatant properties of sand began to change significantly as the proportion of clay added to it increased to 30%, while Lupini *et al*. (1981) showed a sudden difference in residual frictional properties amongst a wide range of natural sediments where the clay content was greater than 35%. Kumar & Muir Wood (1997) described the behaviour of artificial sand–clay mixtures. In those with clay contents above 40% by volume, the clay component determined the strain response, while for those with clay content below 40%, the sand component determined the response. In sand, interparticle contacts mobilize substantial friction,

Downloaded from rsta.royalsocietypublishing.org

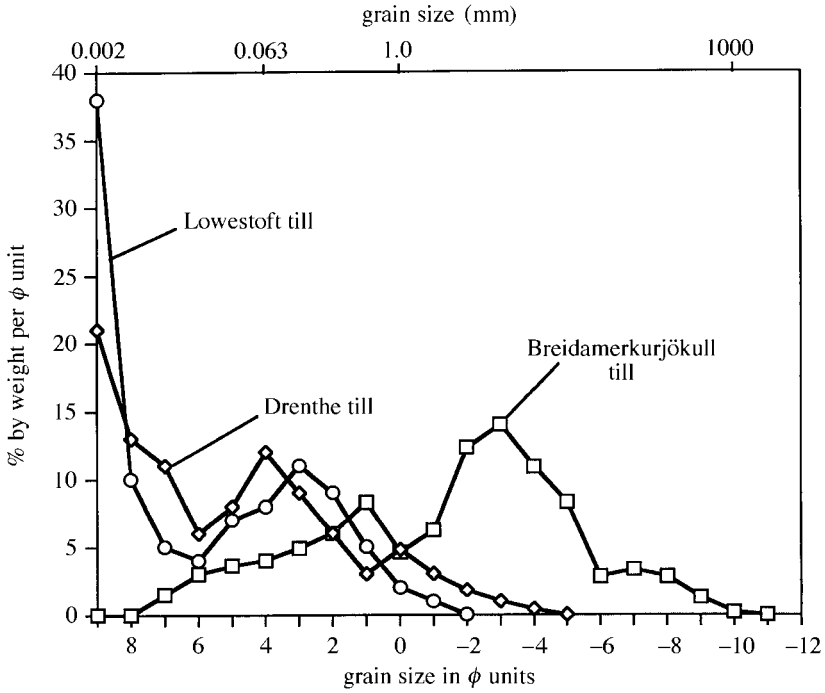

Figure 5. Typical examples of grain size distributions of tills. The Breidamerkurjökull Till is typical of the sandy tills produced by erosion of igneous bedrock. Mineral grains can be assumed to be elastic. The Drenthe and Lowestoft Tills are typical of those eroded from pre-existing sediments in lowland areas. They contain significant proportions of clay mineral grains which we assume to exhibit elastic-plastic behaviour.

whereas it has been suggested that in poorly sorted water-saturated materials, such as the Lowestoft Till (figure 5), the silt and clay fraction behaves as part of the intergranular fluid (O'Brien & Julian 1988; Coussot & Piau 1995). For particularly coarse-grained materials, such as the Breidamerkurjökull till (figure 5), Winter *et al.* (1998) have shown experimentally that, as the concentration of clasts greater than 20 mm in diameter in sandy tills exceeds about 35%, the load is progressively born by interconnecting clasts rather than matrix.

Kamb (1991) analysed a clay-rich till from Antarctica and argued that a highly nonlinear relationship between shear strain and stress was likely, with an exponent of about 100 (class A behaviour). However, Kamb also appeared to presume that such behaviour is an intrinsic property of tills in general rather than of one extreme clay-rich variant. In fact, field and laboratory experiments suggest that the granulometric variability of tills is reflected by a wide range of effective viscosities between about 10^{-8} Pa s^{-1} (Humphrey *et al.* 1993) to 10^{-11} Pa s^{-1} (Jenson *et al.* 1996).

(*b*) *System attributes*

Key attributes of the subglacial system that will influence the rheological behaviour of till are the extent to which movement of a glacier is coupled to its till substratum and the distribution and temporal variation of effective pressure determined by the subglacial drainage regime (figure 4).

Downloaded from rsta.royalsocietypublishing.org

In order to understand the general *behaviour* of till at the base of a glacier therefore, we need to understand both its intrinsic properties and the nature of the subglacial system, in particular its drainage. Although it is interesting to explore the implications of a deforming bed by modelling a system numerically in which the subglacial till has a fixed rheology, as MacAyeal (1992) has done, it is, on an ice-sheet scale, the coupling between the rheology of subglacial sediments of varying granulometry, ice rheology and drainage organization which is the central problem (figure 4). This implies a scale effect. On the very small scale of a laboratory experiment or a highly constrained small-scale field experiment, we might expect to be able to determine relationships between stress, strain rate and effective pressure, which are *intrinsic properties* of the till (e.g. Boulton & Hindmarsh 1987; Clarke 1987). On scales of hundreds of metres, and the very large scales of ice sheets, till behaviour is more likely to be a *system property*, reflecting coupling between till rheology, ice rheology and the structure and efficiency of the drainage system.

We now explore evidence for the deformational behaviour of tills as continua, recognizing that their continuum behaviour in each setting will reflect intrinsic properties and properties of the system which we observe. We present evidence from

controlled laboratory experiments and field experiments, which probably come closest to reflecting intrinsic soil properties;

observations which reflect temporal and spatial variations in patterns of subglacial strain;

natural subglacial field experiments;

large-scale glacial geology, which reflects large-scale system coupling.

4. Controlled experiments

Carefully controlled laboratory experimentation should, in principle, be the means whereby intrinsic shear deformational properties of granular materials are established. Glacial tills pose two problems for such experiments. Firstly, experiments in classical soil mechanics have been primarily designed to investigate failure processes and not the subsequent flow, and as a consequence have been restricted to relatively small strains (typically less than 10%). Secondly, the necessarily small size of experimental devices limits the maximum grain size of the test sample to a few millimetres, which for many tills will require that a large proportion of the grain size spectrum (as much as 30–40% in the example of the coarsest tills in figure 5) is removed from the sample before testing. The first problem can be addressed by using ring shear boxes, although such geometries artificially constrain the pattern of sediment deformation and produce complex distributions of stress which are difficult to measure. The second can be addressed by very large-scale cylindrical (viscosimeter) tests, although they are inevitably limited to analysis of low-density slurries because of the difficulty of generating the large stresses which would be required to cause deformation in denser materials. We first review experiments on materials which have granulometric similarities to glacial tills and then report on experiments on tills.

Downloaded from rsta.royalsocietypublishing.org

Table 1. *Remoulded soil types*

soil	soil character	flow law exponent
London clay	silty clay	6.4 (standard deviation 2.76)
Forties clay	silty clay	4.84 (1.59)
Magnus clay[a]	silty clay with some gravel and shell fragments	2.63 (0.46)

[a]The Magnus clay is similar to many fine grained tills.

Experiments have explored two regimes: a low strain rate regime in which slow non-inertial intergranular contacts dominate, and a high strain rate regime in which inertial grain collisions become important.

In relatively small strain, confined uniaxial compression tests involving non-inertial contacts in clay soils, it has been conventional to distinguish between primary and secondary compression (Taylor & Merchant 1940). Primary compression depends upon the rate at which water is expelled from voids between clay mineral packages (Terzaghi 1925) and leads to a state in which effective stress is in equilibrium with the load. Secondary compression, which appears as viscous creep, is much slower, continuing after primary compression is complete, and was predicted to be highly nonlinear by Taylor (1942). A non-Newtonian structural viscosity in clay soils was predicted from rheological considerations by Rosenqvist (1963) and demonstrated experimentally by Schmid *et al*. (1960). Internal structure had long been considered by rheologists to be the source of an apparent nonlinear viscosity, characterized by a simple power law, $\dot{\varepsilon} = k\tau^n$ (Wilkinson 1960). Barden (1965) demonstrated a power law exponent of $n = 5$ for a saturated clay in a compression test. It is presumed that after the disruption to structure caused by primary consolidation, clay particles pass from a solid to a 'lubricated' state (Terzaghi 1941), and that stress is progressively transferred from the lubricated fluid to the solid as equilibration occurs. Shear strains, however, will tend continuously to disrupt structure and thereby to maintain a creep response.

Experiments designed to explore the frictional resistance associated with the driving of piles into soils yield information about larger, faster strains. Heerema (1979) showed that friction at the side of a pile is very strongly velocity dependent at low velocities and relatively insensitive at high velocities. Experimental simulation of pile driving by Litkouhi & Poskitt (1980) showed that a nonlinearly viscous law relating shear stress and strain rate was appropriate for a wide range of soils. They tested three remoulded soil types for velocities in the range 0.05–1.5 m s^{-1} as shown in table 1.

A strong theme of theoretical and experimental work has been inspired by Bagnold's (1954) analogy between the collisions of particles in a grain flow and the kinetic theory of gases (Maxwell 1866; Boltzmann 1896), which led him correctly to predict the shear strain rate dependence of shear and normal stress in collisional flows. In many geological phenomena, there is an interplay between the intergranular friction typical of slow flows and the collisional behaviour which dominates in fast flows, although most theoretical and experimental work has addressed the latter. Subglacial deformation belongs to the slow flow regime.

Savage & Sayed (1984) conducted experiments on rapid shearing of dry granular materials with a grain diameter of about 1 mm, in a ring shear apparatus at relatively

Downloaded from rsta.royalsocietypublishing.org

high solids concentrations ($n = 0.5$) but at very high shear strain rates of the order of 5 s^{-1}, many orders of magnitude greater than in subglacial tills. They showed that stresses were proportional to the shear strain rate raised to a power less than two. Johnson & Jackson (1987) developed constitutive relationships for such a shearing mass involving both short duration inelastic collisions and semi-permanent frictional contacts in which shear and normal stresses are functions of the shear strain rate. They analysed the transition between an upper rapidly shearing collisional regime with high granular temperatures and a lower progressively more frictional regime with near zero granular temperatures. In a sloping long-flume, free-surface experiment with 6 mm plastic spheres monitored by high-speed camera, Drake (1990) clearly observed this interface and the details of particle interactions. The lower, frictional zone was highly structured, in contrast with the structureless collisional zone, with slowly deforming and mutually interacting block-like domains overlain by a zone of grain-layer gliding. On a rough bed, there was little slip at the base but there was strong shear strain in the frictional zone of the order of 10 s^{-1}. On the smooth bed on which sliding took place, there was little or no shear strain in the lower part of the frictional zone.

Phillips & Davies (1991) tested debris flow material in a 2 m diameter viscosimeter at shear strain rates between 2 and 15 s^{-1}. They found that apparent viscosities were shear rate dependent and extremely sensitive to water content. For sediment with a modal grain size of about 0.2 mm (fine sand), they found nonlinear relationships of $\dot{\varepsilon} = k\tau^{2.95}$, and for a sediment with a modal grain size of between 0.5 and 1 mm (coarse sand), they found linear relationships between shear stress and strain rate (compare modal grain sizes with those of the tills in figure 5).

Wong *et al*. (1995) subjected a silty, clayey sand from a landslide to a consolidated, drained triaxial test and a stress-controlled strain rate test to estimate viscoplastic parameters, which showed results giving equivalents to the exponent n in equation (2.4) of 1.16, 2.97, 0.51 and 2.15. These values were found to be compatible with the measured strain profile in the landslide using Iverson's (1985) expression for the velocity distribution in a shear zone.

In order to establish whether shear stress and effective normal stress remain strain rate dependent at shear strain rates similar to those found in a subglacial setting, we have undertaken a series of experiments to explore the relationships between stress and strain rates and effective pressure for a till matrix undergoing large shear strains at slow rates, by using a standard ring shear apparatus. The sample is annular with a depth of 20 mm or 40 mm, a width of 25 mm and a maximum annular diameter of 150–200 mm. The plane of shear is horizontal. Shear stresses and strains were calculated by using assumptions discussed by Bishop *et al*. (1971). Tests were undertaken for a range of loads normal to the plane of shear and for a range of displacement rates between about 1 and 1000 m a^{-1}, held constant for each test. Variations in shear stress were measured during the tests. It was found that the same residual friction was produced after significant displacement irrespective of whether tests were undertaken on pre-consolidated or remoulded samples, showing that at large deformations at least, there is no cohesion. Before shear testing, normal loads were applied until primary consolidation had ceased. In most cases, it was found that there was a residual stress which was significantly less than the peak stress attained early in the test (figure 6). After calibration against a standard of Speswhite kaolin, two tills were tested:

Downloaded from rsta.royalsocietypublishing.org

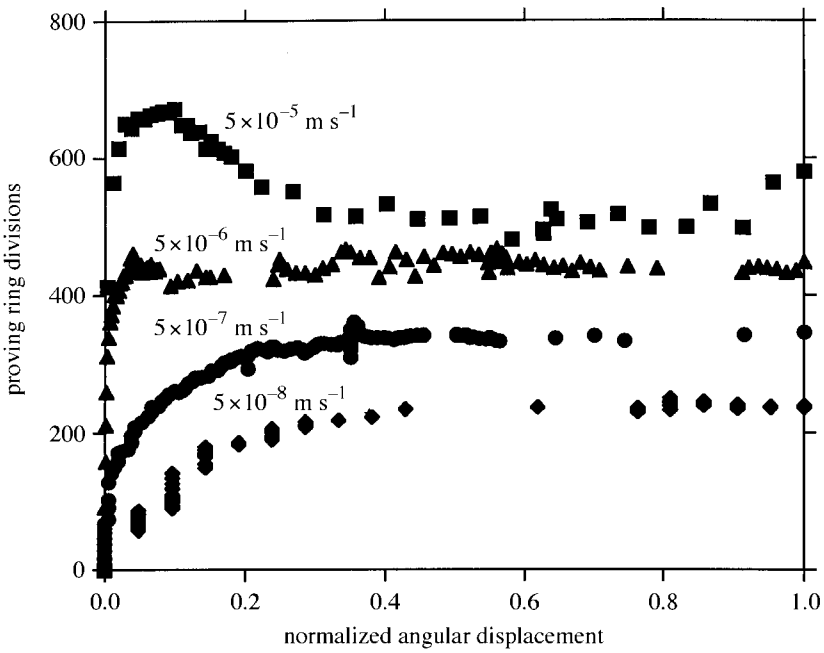

Figure 6. Shear resistance in proving ring divisions plotted against normalized angular displacement for different values of displacement rate for Drenthe Till samples. Note that higher shear resistance is generated by higher displacement rates. The clear contrast between peak and residual shear strengths for more rapidly deforming materials is associated with significant dilation. Tests at higher confining pressures also produce larger dilation.

Drenthe Till A clayey-silt till (25% clay content) from The Netherlands. A typical grain size distribution is shown in figure 5. The sample depth was 20 mm. The fine-grained nature of the till made it possible to use a carefully selected, remoulded sample without having to sieve out coarse grains. At the end of the test, an irregular shear zone of increased water content was observed which was 2–3 mm in thickness. Finite shear strains were calculated from the width of this zone.

The tests showed that the shearing resistance is influenced by the rate of shear strain (figure 6), a result which was also obtained by Lupini (1981) from ring shear tests on clays. Triplets of measurements for each sample of Drenthe Till permitted relationships between displacement rates, effective pressures and shear stresses to be determined. These tests effectively determined the shear resistance of the till to a given rate of displacement and for a given confining pressure. We assume that this relationship can be inverted to give the strain rate for a given shear stress. We then estimate parameters n and m in equation (2.5), which, for the Drenthe Till, are $n = 13.7$, $m = 15.9$.

Breidamerkurjökull Till A sandy till from one of the sites in Iceland at which the field experiments analysed by Boulton & Hindmarsh (1987) were undertaken. In these experiments, the annular diameter of the cell was 200 mm and the sample depth was 40 mm. A series of thin, 2 mm deep plates, which extended across the radial width of the cell were attached to its upper and lower surfaces to prevent

Downloaded from rsta.royalsocietypublishing.org

slip at those surfaces. In view of the coarse grain size of the matrix, the sample was sieved to remove all grains greater than 5 mm in diameter. It was, however, possible to find relatively large areas of matrix in which there were few grains in excess of this diameter. During tests, variations of shear stress were significantly greater than in the case of the Drenthe Till, which we attribute to the greater variation of grain size in the Breidamerkurjökull Till and greater blocking of strain through interactions between larger grains and the formation of multi-grain domains similar to those observed by Drake (1990). Although the ring shear box forces a narrow shear zone to develop between the two halves of the box, it is more difficult to form a narrow zone in a coarse sediment, so that shear-zone thickness is partly controlled by grain size. On inspection after testing, it was found that the thickness of the low density shear zone was between 6 and 11 mm. Roscoe (1970) has argued that the dilated layer produced by localization of strain within a sediment should be about 10–20 grain diameters in thickness. In the examples shown in figure 7, where the modal diameter was about 0.5 mm, it would predict a dilation zone thickness of 10–20 mm, compared with the actual thickness of 6–11 mm. The tests with higher displacement rates and with smaller normal stresses tended to show thicker shear zones. Tests in which carefully emplaced vertical arrays of 2 mm diameter iron pellets were used as strain markers by X-raying the sample after 80 mm of displacement (figure 7), showed that the zone of shear was significantly thicker than the dilated zone, that significant vertical dispersion between markers occurred in the dilated zone and, from X-ray images of the horizontal plane, that significant horizontal dispersion also occurred. We suggest that this was a consequence of the fact that there is a radially outwards increase in the rate of shear, which will produce radial contrasts in dilation and thus generate lateral grain mobility. The X-ray imaged thickness of the dilated zone is therefore likely to be the maximum thickness near the outer wall of the cell.

Experiments on the Breidamerkurjökull Till were primarily concerned with the geometry of strain and involved only a small number of tests. It is noticeable, however, that the sieved laboratory sample of the Breidamerkurjökull Till was softer than the apparent behaviour of the till in the field experiment. This may reflect the absence in the laboratory test of the large fraction coarser than 5 mm, or it may reflect properties of the subglacial setting which cannot be simulated in the laboratory.

The results of our experiments appear generally to conform to the conclusions of other laboratory tests, that a power law is a good general descriptor of the relationship between strain rate and shear stress, although it is difficult numerically to compare rheologies which have been obtained from such very different experiments. The sandy, bouldery Breidamerkurjökull Till shows a weakly nonlinear behaviour of class B, while the silt- and clay-rich Drenthe Till shows a strongly nonlinear behaviour of class A. In this regard (figure 2*b*) it is interesting to note that the Drenthe Till is very thin in the northern Netherlands.

5. Field observations of patterns of strain

Although our principal concern is with the slow strain-rate behaviour of granular materials in the subglacial environment, it is useful to make comparisons with observed patterns of strain in unconfined debris flows, particularly because such flows often include a wide range of poorly sorted grain sizes similar to that typical of till.

Downloaded from rsta.royalsocietypublishing.org

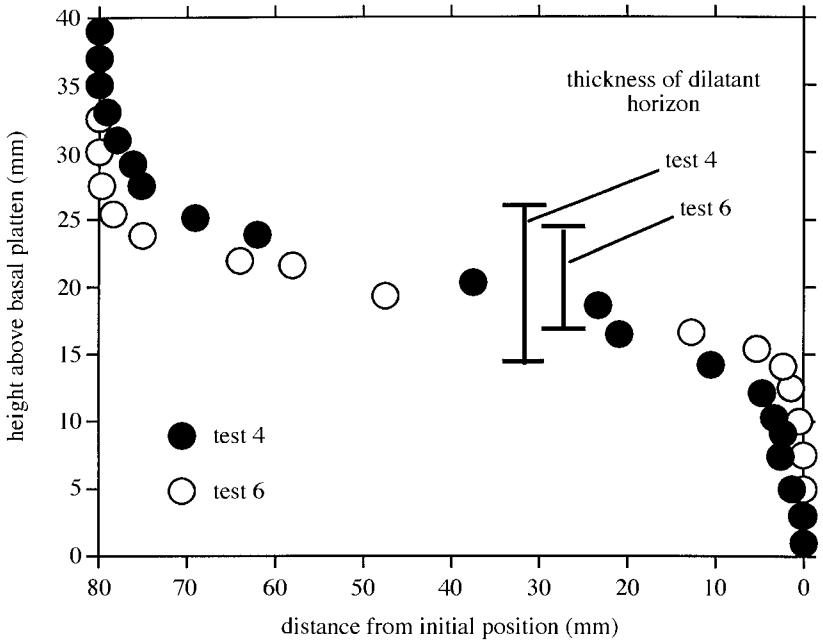

Figure 7. Reconstruction from X-ray images of the displacement of 2 mm iron pellets in Breidamerkurjökull Till after 80 mm of shear displacement. The plane is vertical and parallel to the direction of shearing in the annular shear box. The pellets were initially emplaced in a vertical column. The dilated horizon was also recorded on X-ray images, but could be seen clearly by eye when the sample was taken from the shear box. Images in the horizontal plane showed significant lateral (radial) displacement of pellets. The thickness of the dilatant horizon was inferred from density contrasts on X-ray images.

Debris flows show a combination of low flow rates with enduring frictional contacts and more rapid collisional flow modes. They show evidence of flow instability in rapid surges and the development of compressional waves (Iverson 1997). Profiles of velocity with depth in slow, non-inertial flows have been used to estimate values of n in equation (2.5) of between 1 and 3 (Savage & Cheleborad 1982; Swanston *et al.* 1983; Iverson 1985).

Similar patterns of strain, measured in field experiments beneath the glacier Breidamerkurjökull in southeast Iceland, are shown in figure 8, although the strain pattern is inverted compared with debris flows. Shear strain increases upwards towards the major shear plane represented by the glacier sole, while in the case of a debris flow, shear strain increases downwards towards the basal shear plane of the flow. The displacement of remotely inserted strain markers in the subglacial till at Breidamerkurjökull over periods of up to 9 days suggested values of n of between 1.3 and 2.4, and showed shear strain rates immediately beneath the glacier sole of between 35 and 80 a^{-1}. This strongly deforming horizon overlaid an apparently stable till horizon. Measurements at a series of sites of average (though strongly fluctuating) water pressures, cumulative strains and calculation of shear stresses led to the fitted flow rules in equations (3.1) and (3.2). The zone of high apparent shear strain is also one in which voids ratios are high (between 0.55 and 0.65) compared with the

Downloaded from rsta.royalsocietypublishing.org

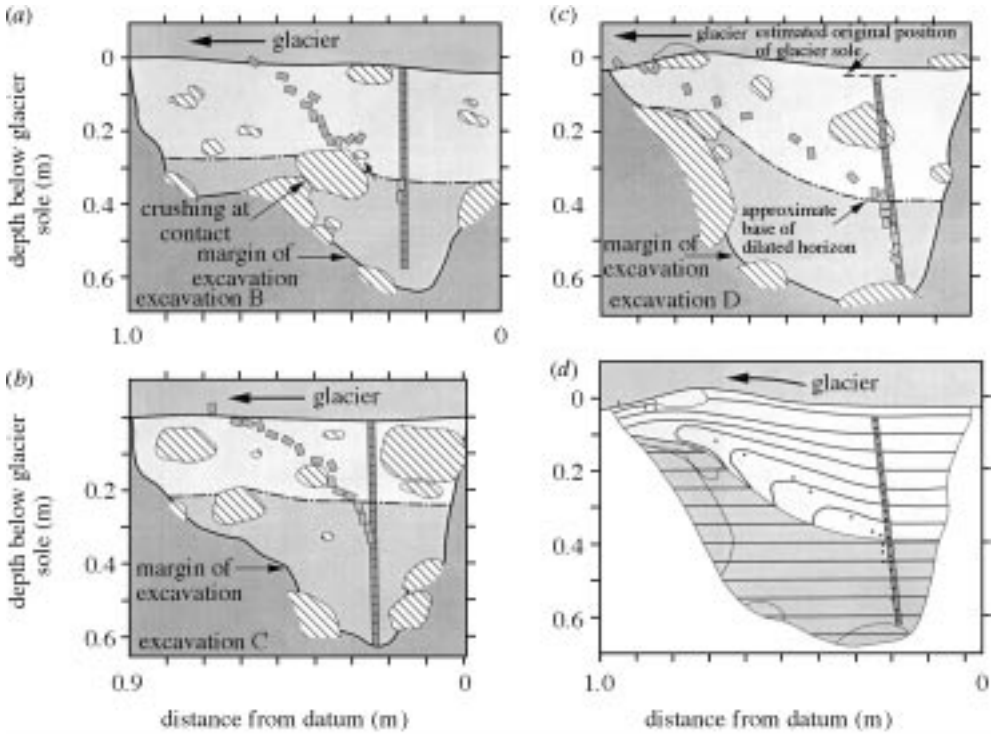

Figure 8. Pattern of strain in till beneath Breidamerkurjökull shown from the displacement of strain markers (1977/78 experiments) at three sites (*a*)–(*c*). The pattern of flow in (*c*) is one that would show as folding in a stratified sediment, because of the locally upward trajectory of flow over the large blocking boulder. (*d*) shows how an initially horizontally stratified sediment would be folded by the pattern of displacement shown by strain markers.

underlying more stable horizon (0.4 to 0.5), which we presume to result from dilation in the deforming horizon.

Similar strain profiles have also been measured by Blake & Clarke (1992, fig. 5) beneath the Trapridge Glacier in Canada by using a string of sensors which show shear strain rates of about 30–50 a^{-1} through a 0.2 m thickness of till immediately beneath the glacier sole (although the physical linking of transducers may restrain the movement of some, particularly where strain rates are high near to the glacier sole).

The movement of strain markers shows that the pattern of strain is not restricted to movement along planes of shear parallel to the glacier sole. If, for the example shown in figure 8*c*, we imagine horizontal strata in the till at the commencement of the experiment, figure 8*d* shows how they would have been deformed by the pattern of strain reflected in the movement of the strain markers. The apparent fold is generated by a transient strain trajectory oblique to the dominant planes of shear. It is clearly produced as a result of blocking of flow in the deforming horizon by boulders which are deeply embedded in the underlying stable horizon so that the flow is forced to rise over the boulders.

Folds which reflect such a pattern of flow are ubiquitous in tills and sediments which have bedding and lamination, and which are thereby able to reflect folding.

Downloaded from rsta.royalsocietypublishing.org

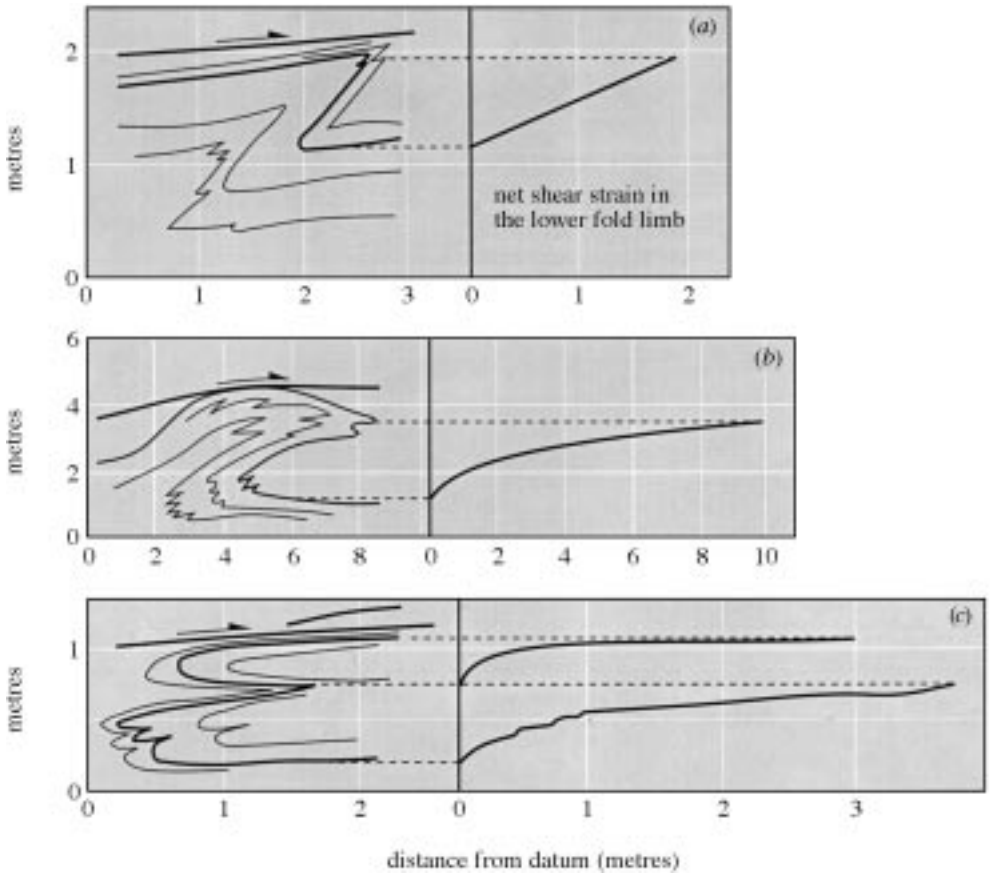

Figure 9. Examples of folds produced by deformation of sediments beneath a glacier sole and the inferred strain in their overturned limbs. To the right of each field sketch is shown the net shear strain in the lower, overturned limb of the fold. In case (*c*), where an upper fold has been superimposed upon a pre-existing fold, the strain is shown separately for each fold. In reality, the second phase of strain adds to that of the first. (*a*) A fold in sands beneath the Drenthe Till in the northern Netherlands. (*b*) A fold in sands beneath an upper Ordovician glaciated surface in Saudi Arabia. (*c*) Complex folding in a stratified sand–silt–clay sequence beneath the Anglian till near Ipswich in eastern England. Note that the direction of glacier movement is from left to right in each case and that the surface of glacier overriding is shown by the heavy line immediately beneath the arrow.

Figure 9 shows folds typical of sediments which have lain immediately beneath a moving glacier sole. Such folds in stratified materials are produced wherever the flow trajectory is oblique to the dominant plane of stratification. The strain associated with generation of the folds can be approximately recovered by making the reasonable assumption that the bed was horizontal immediately before folding and that relatively little longitudinal compression or extension occurred in the plane of the bed during the folding episode compared with simple shear deformation. The localized relative velocity profiles inferred from such folds are illustrated in figure 9*a–c* for examples which show progressively greater shear strain. The enhanced strain is located in the upper limb of the synclinal fold closure, and is superimposed upon

Downloaded from rsta.royalsocietypublishing.org

any pre-existing pattern of strain. The flow rule exponents compatible with these patterns of strain can be deduced from the rule suggested by Iverson (1985) and lie in the range of about $n = 2$–5. These patterns of strain also explain the extreme shear thinning which appears to be characteristic of till folds and is reflected in the upper limbs of the double fold in figure 9*c*. We conclude that the styles of many folds observed in sediments which have undergone shear deformation beneath the sole of a glacier reflect class B behaviour with a relatively small exponent nonlinear strain response to stress.

Folding episodes represent local and temporary stress concentrations. Observations at Breidamerkurjökull suggest that episodes of folding are associated with irregularities on the interface between the deforming and stable horizons. Observations of this interface, where it is exposed beyond the glacier, suggest that such irregularities are common, with typical spacings of a few metres. However, folds also seem to occur where there are no irregularities on the underlying surface, suggesting that the till becomes locally stiff, probably because of locally good drainage and low water pressures, produced by granulometric contrasts or hydraulic events. They probably reflect a temporal change in the mosaic of stress, and suggest that compressional waves and instabilities are as common in deforming tills as they are in debris flows. As the velocity of the upper part of the deforming horizon at Breidamerkurjökull was of the order of 20 m per year, any element of till might expect to suffer about 10–20 major folding episodes per year. This has two implications.

1. The frequency of folding episodes will contribute to the average rheological behaviour of the deforming bed. They are stress concentration events during which strain is blocked by stiffness in the system, created either by irregularities on the base of the deforming horizon or deforming sediment masses of different strength (different granulometry or different local effective stress conditions). The irregularity of the sheared zone in the laboratory test of the sieved Breidamerkurjökull Till reflects, on a much smaller scale, similar blocking events.

2. The folding episodes, followed by the shear thinning and attenuation produced by the overall regime of shear strain, will tend to mix and homogenize all the strata which are involved in folding, eventually producing a homogenized till unit (e.g. Hart & Boulton 1991). Boulton (1987) has suggested that the creation of such a homogenized till stratum acts to facilitate adjustment of a glacier to its bed during flow and to reduce the frequency of granulometrically generated stress concentrations, although hydraulic events may still produce them.

Observations of patterns of strain in subglacial sediments also reveal complex three-dimensional strain geometries. For example, upward extrusion flow of till is produced in the lee of relatively more stable, deeply embedded boulders an extrusion flow which then propagates down-glacier to generate linear flow marks, termed ‘flutes’, on the till surface (see, for example, Paul & Evans 1974).

6. Field experiments to monitor deformation

Laboratory limitations on the magnitude of stress, strain and grain size make monitoring of natural field experiments attractive. The first experiments to evaluate *in situ* subglacial rheological properties were undertaken by Boulton & Jones (1979)

Downloaded from rsta.royalsocietypublishing.org

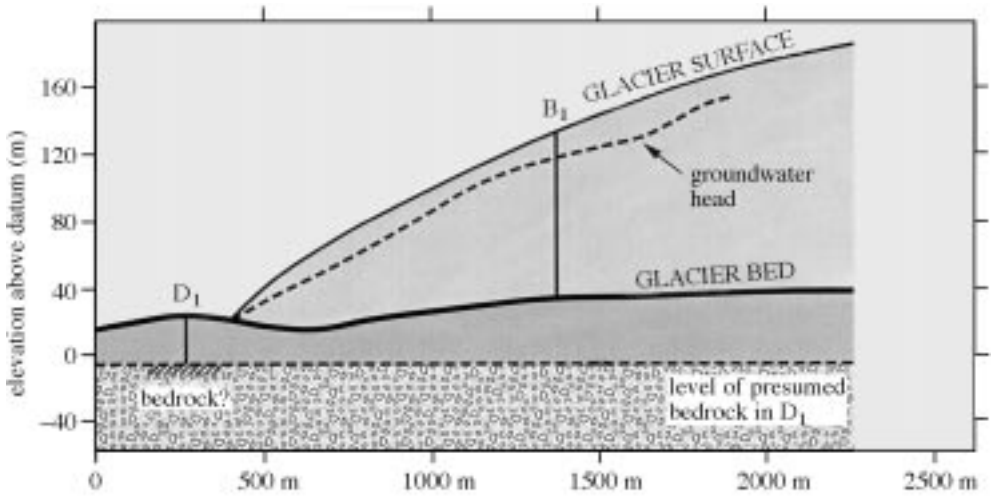

Figure 10. Flow-parallel cross-section through the terminal zone of Breidamerkurjökull showing the profile of the glacier surface and the location of borehole (B1) at the base of which the reported strain measurements were made. The form of the ice–bed interface was inferred from a radio-echo survey. A seismic survey in the proglacial zone (Bógadottir *et al*. 1985), validated in part by borehole D1, shows a roughly horizontal bedrock surface overlain by a thick sand and gravel unit. This sequence has been projected beneath the glacier. The groundwater head at the top of the sand and gravel aquifer is interpolated from measurements on day 253 between borehole B1 and others in the vicinity. A till unit, normally about 1 m thick, forms a low permeability layer between the glacier sole and the aquifer. It is within this unit that the large shear strains shown in figure 13 are concentrated. Very little deformation is thought to occur in the sand and gravel aquifer.

beneath ice no thicker than 7 m near to a glacier margin (cf. figure 10). The purpose was to use this setting as a natural shear box which would avoid the limitations of laboratory experiments, not to investigate a site that was representative of subglacial conditions (we still do not know what representativeness would require). The drawbacks of the approach were the following.

Only the net strain at the end of the experiment could be measured, which was then correlated with average shear stress and average effective pressure at each experimental site, approximations which produced highly smoothed relationships.

Shear stress was taken to be the direct gravitational stress at the site, there being no practicable way of measuring or calculating the longitudinal stress.

In the event, diurnal fluctuations of subglacial water pressure were found to occur, a system characteristic which Boulton & Hindmarsh (1987) showed would significantly influence the dynamics of strain response. This partly invalidated the objective of the experiment to determine material properties which were independent of the specific setting.

Even though we now conclude that such field experiments can only yield measures of till behaviour as a product of material properties and setting, the site has great

Downloaded from rsta.royalsocietypublishing.org

advantages. It is known that the glacier rests, over a large area, on a flat surface of relatively thick till whose *in situ* characteristics and stratigraphic setting are known (figure 10).

Some subsequent experiments made under thicker ice underlain by till (e.g. Kamb 1991; Iverson *et al.* 1995) have suggested that the *in situ* shear strength of till at these locations is too small to support the glacier shear stress, and thus that the till must occur in basins lying between more resistant, possibly bedrock, eminences which support proportionately more of the stress, underlining the need for greater knowledge of the subglacial setting in interpreting results.

Experiments by Blake & Clarke (1992), Blake *et al.* (1992) and Iverson *et al.* (1995) have involved remote insertion into the bed, from the base of boreholes, of strings of tilt meters, from which patterns of strain have been inferred from the rotation of individual tilt meters. Their drawback is revealed by inspection of figure 8 (see also Boulton & Jones 1979), which shows how different patterns of rotation between adjacent cylindrical strain markers are a consequence of locally complex patterns of flow rather than a reflection of larger-scale patterns of shear strain in the till. Physical connections between arrays of tilt cells are likely to exacerbate this problem.

In order to avoid these problems, a series of independent strain markers were inserted into subglacial till at Breidamerkurjökull from the bases of several boreholes which penetrated to the bed, with the intention of monitoring their movement rather than their tilt. A similar experiment was undertaken by Boulton & Hindmarsh (1987) and Blake *et al.* (1994), although the latter used only a single marker. The strain markers incorporated water pressure sensors, and were individually attached by wire to free running spools in oil-pressurized cylinders which blocked the base of the boreholes at the ice base. The rotation of the spools was measured by potentiometer. The experiments reported by Boulton & Hindmarsh (1987) had demonstrated that strain measured by wire and strain marker gave results which agreed with direct observations of cumulative strain.

The site of the most successful experiment, at borehole B1b, is shown in figure 10. Strain markers were emplaced at the level of the glacier sole (T_0) and at depths of 0.1 m ($T_{0.1}$), 0.3 m ($T_{0.3}$), 0.5 m ($T_{0.5}$) and 1.0 m (T_1) below the glacier sole beneath an average ice thickness of 105 m. Continuous records of the spooling out of the wires for all strain markers were obtained for a period of 17 days. The principal uncertainty in interpretation is whether the transducers move relative to the till in which they lie and whether the wire forms a direct or indirect trajectory between transducer and spool (cf. Blake *et al.* 1994). Attempts to test wire and transducer behaviour were made by emplacing transducers and connecting wires in till beyond the glacier which was then artificially slumped at effective pressures very little different from those which obtained during the subglacial experiments. It was found that transducers did move with the till and that straight wire connections were maintained, except when the wire was deflected around boulders in the flowing till. As the records of different strain markers in the experiment reported here are mutually consistent, we shall assume that straight connections were maintained, although this cannot be clearly demonstrated, and some distinctive features of the records of individual markers may be a result of deflections of wires around clasts.

The absolute movement of the sensor at the base of the borehole was estimated from a survey of the top of the borehole from an extra-glacial position, accurate to within 8 mm, and a borehole inclinometer survey with a potential error of up to

Downloaded from rsta.royalsocietypublishing.org

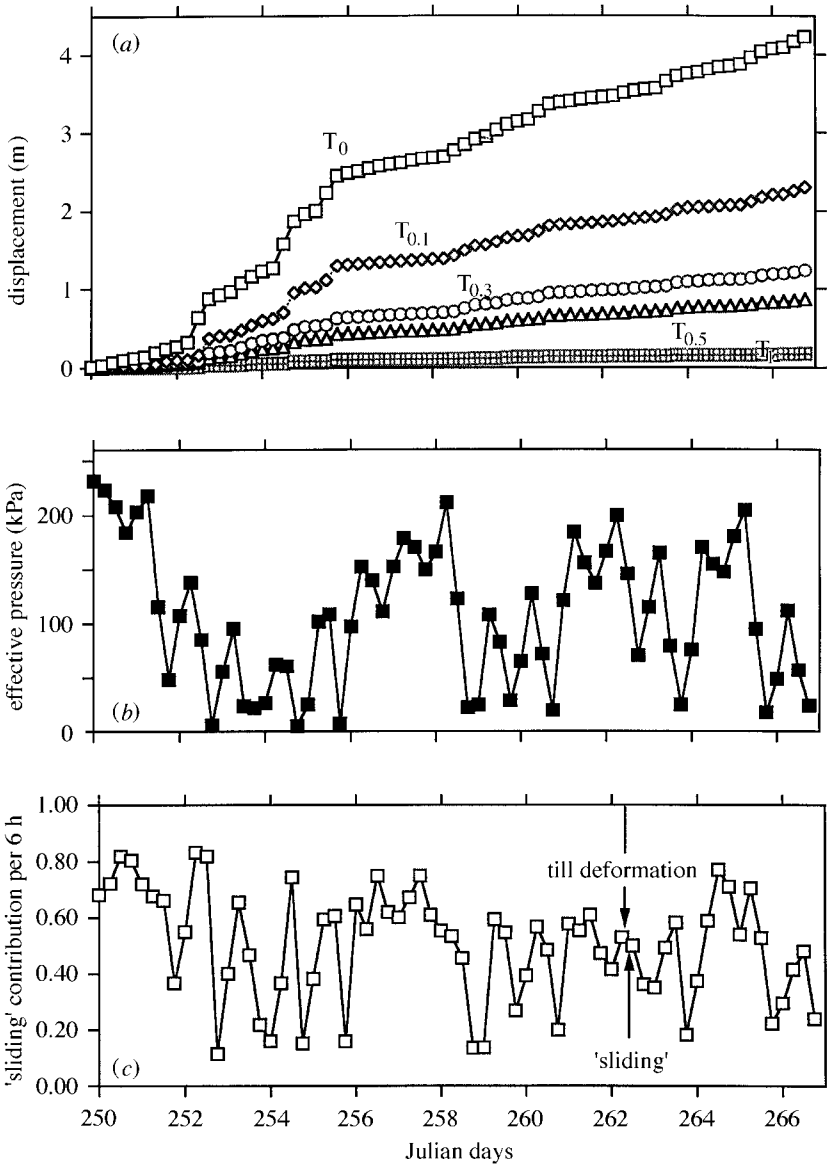

Figure 11. Subglacial experiment at Breidamerkurjökull. (*a*) Displacement of the transducer series during a 17-day experiment. (*b*) Effective pressures at the level of transducer $T_{0.1}$ at 6 h intervals calculated from measurements of water pressures. (*c*) The proportion of the movement of the glacier sole due to sliding and to till deformation. The former is estimated from T_0–$T_{0.1}$, the latter from $T_{0.1}$–$T_{0.3}$.

35 mm. It is estimated that the cumulative displacement of the 1.0 m sensor (T_1) was 0.176 ± 0.043 m during the period of the experiment. Within this bound, it was assumed that the daily displacement of this sensor was proportional to the relative motion between this and transducer ($T_{0.5}$). From this we estimate the absolute movements of other transducers.

Downloaded from rsta.royalsocietypublishing.org

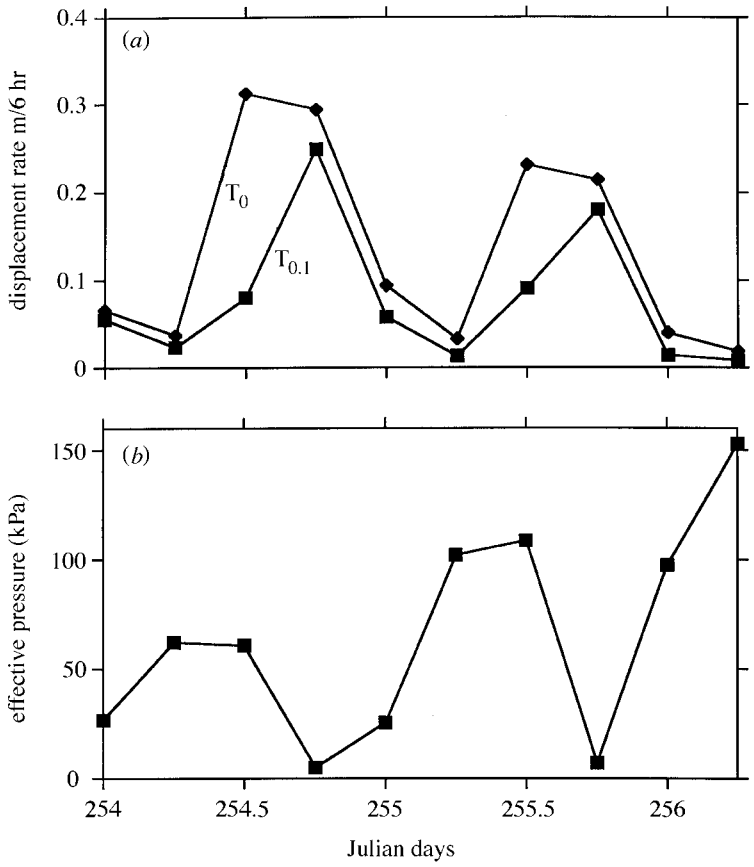

Figure 12. (*a*) Displacement rate for transducers T_0 and $T_{0.1}$ and (*b*) effective pressures at $T_{0.1}$ for a 54 h period. T_0 is located in the basal ice and $T_{0.1}$ is located in the till, 0.1 m below the glacier sole. Note that peak rates of basal ice displacement are reached before those for the topmost till transducer and that although there is a general association between low effective pressure and high displacement rate, there is not a strong linear correlation. We suspect that stick-slip behaviour at the ice–bed interface, and complex till stratum dynamics, as suggested in figure 15, may be the cause.

Strong diurnal oscillations of water pressure were measured by the transducers. The effective pressure fluctuations shown in figure 11*b* were derived by subtracting water pressure values from the pressure due to the thickness of overlying ice, which varied by less than 3 m during the period. The water pressure variations appear to be driven primarily by water pressure oscillations in the underlying aquifer (figure 10). High water pressures are maintained by melting of ice at the base of the glacier, which remains roughly constant through the year, and by surface meltwater which is diurnally injected during the melting season down crevasses and moulins which penetrate to the bed. These point injection sources appear diurnally and rapidly to pump up water pressures in the highly transmissive sub-till aquifer, which produces fluctuating water pressures at the base of the till.

Downloaded from rsta.royalsocietypublishing.org

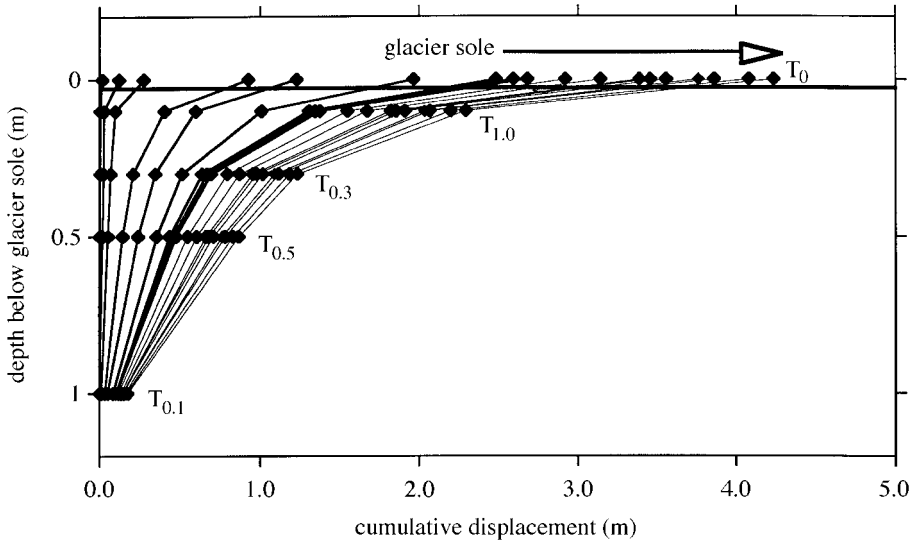

Figure 13. Reconstructed pattern of daily displacement of transducers during the Breidamerkurjökull subglacial experiment. It is difficult to assess the extent to which the relative displacement between transducers T_0 and $T_{0.1}$ reflects sliding at the ice–bed interface or deformation in the till. In figure 12*c*, it is assumed that a change in the ratio of T_0–$T_{0.1}/T_{0.1}$ reflects their changing contributions.

The inferred six-hourly displacements of sensors for the period of 17 days are shown in figure 11*a*, and compared in figure 11*b* with six-hourly effective pressures at transducer T_0. Figure 12 shows displacement rates of transducers T_0 and $T_{0.1}$, together with effective pressure fluctuations during a 54 h period. Figure 13 shows the vertical profile of cumulative displacement during the whole of the experimental period. Figure 14 shows vertical profiles through the till of water and effective pressure during a 24 h period from the evidence of transducers T_0 to T_1. Figures 11–14 show several important features which are listed below together with the conclusions which we draw from them.

(a) *Variations in rates of displacement of transducers* $T_{0.1}$–$T_{0.5}$ *are generally in phase with each other.*

We suggest that this reflects the flow of a well-defined stratum analogous to the highly dilated masses shown in figure 8 above a relatively stable horizon. However, we do not know whether this takes place through a large number of highly localized shearing events, or as a process of continuous dispersed strain. It seems most likely, from observations of tills exposed beyond the glacier terminus, that the former is dominant in the lower part of the till and the latter is common in the upper part.

(b) *There are several rapid, relatively large, possibly instantaneous displacements of upper till transducers which are not reflected in lower transducers.*

For instance, at 255.25, $T_{0.1}$ shows the beginning of a period of rapid displacement which does not extend to $T_{0.3}$ until at least 6 h later (figure 11*a*). This reflects a pattern in which the base of the rapidly deforming mass moves up

Downloaded from rsta.royalsocietypublishing.org

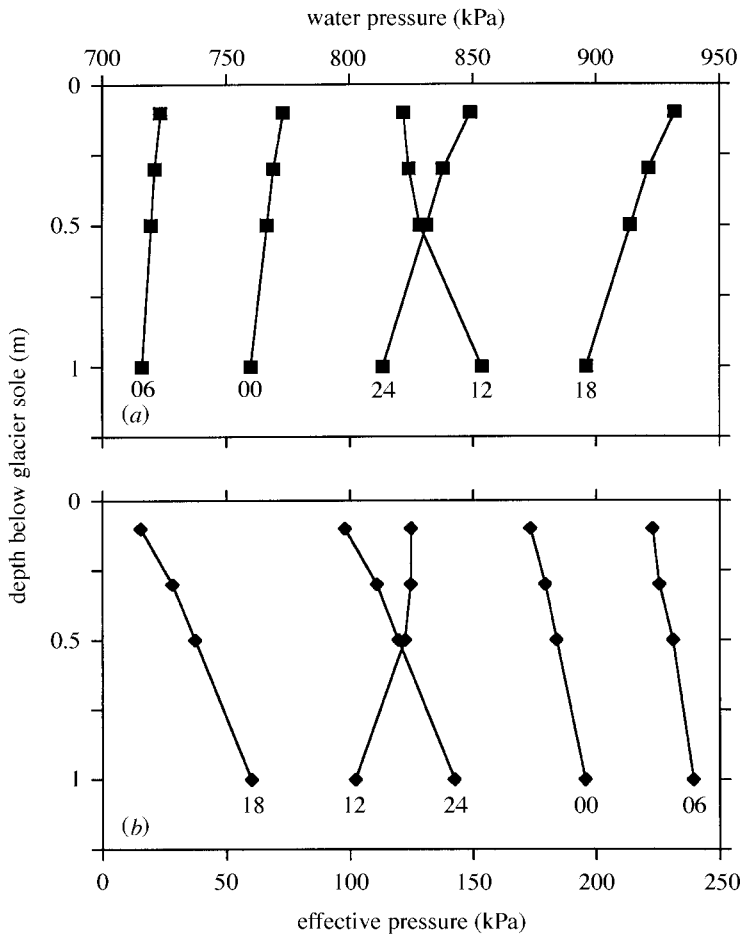

Figure 14. (*a*) Measured water pressures at transducers in the subglacial till during a 24 h period on day 258 of the Breidamerkurjökull experiment. (*b*) Inferred effective pressures.

and down with time, generally associated with fluctuations in effective pressure. The rapid displacement events seem to occur during periods of accelerating flow and diminishing effective pressure when we presume that the upper part of the till responds sooner than the lower part, although the base of active deformation moves downwards. Figure 15 shows the vertical distribution of strain rate in the till as a function of time, showing the way in which the base of the rapidly deforming mass rises and falls, largely in phase with changes in effective pressure within the deforming mass. We presume that such strong temporal variations in the vertical distribution of deformation will tend to be associated with horizontal contrasts in deformation rate. This will arise both from the influence of the till's granulometric inhomogeneity on the pattern of water pressure diffusion and, given the point sources of water injection onto the aquifer, from waves of water pressure change with a strong horizontal component. Horizontal contrasts in the rate of deformation will inevitably give rise to folding episodes of the type shown in figure 8.

Downloaded from rsta.royalsocietypublishing.org

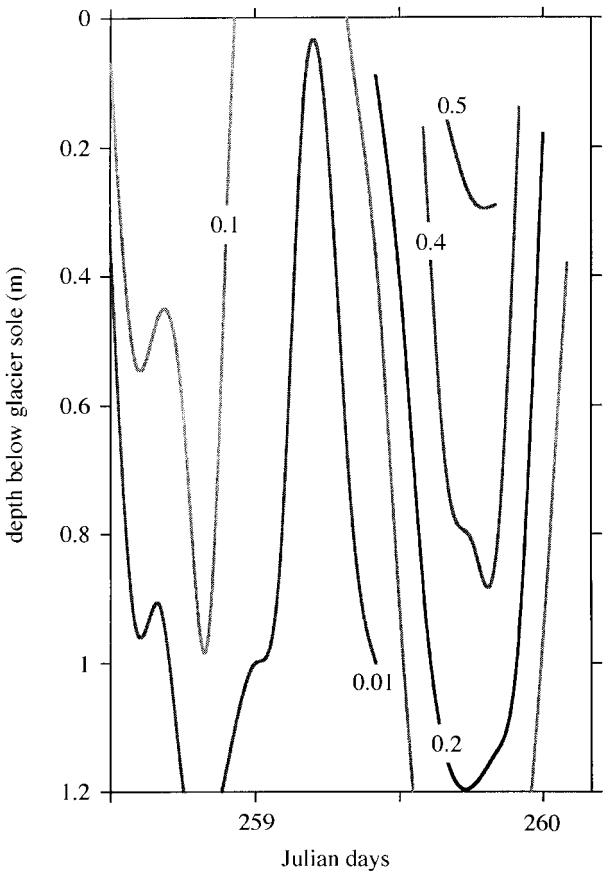

Figure 15. Approximate time-dependent shear strain rate field through the Breidamerkurjökull till during a 40 h period.

(c) *Although the most rapid displacements of transducers tend to occur at periods of low effective pressure, variations in the rate of transducer displacement do not appear to be precisely in phase with effective pressure fluctuations and variations in rates of displacement of transducer* T_0 *do not appear to be precisely in phase with those for transducer* $T_{0.1}$.

Figure 12*a* shows the relative displacement between T_0 and $T_{0.1}$ and between $T_{0.1}$ and $T_{0.3}$ during a 24 h period. They are not in phase. We explain this by suggesting that T_0–$T_{0.1}$ largely reflects slip at the ice–bed interface, while $T_{0.1}$–$T_{0.3}$ reflects the strain rate in the upper part of the till. As effective pressures decrease (figure 12*b*), T_0 accelerates before $T_{0.1}$, and $T_{0.3}$ and decelerates before them and before the effective pressure minimum occurs. It suggests that the ice–bed interface becomes a surface of easy gliding associated with diminished mechanical coupling between the ice and its bed, possibly through extreme softening of the upper surface of the till, which could also permit the glacier sole, with the boulders embedded in it, to plough more readily through the till before till deformation reaches a peak. As the rate of till deformation begins to increase we presume that coupling is re-established, the till softens rapidly and

Downloaded from rsta.royalsocietypublishing.org

at very low effective pressures deforms much more readily than sliding occurs at the ice–bed interface. These observations are similar to those of Drake (1990) that internal deformation in a flowing mass was minimized by easy sliding at its base. Blake *et al.* (1994) may have measured the operation of part of such a system beneath the Trapridge Glacier in Canada, where they noted that the differential velocity between the upper part of a deforming bed and the glacier sole was a maximum during the period of diurnal water pressure increase, but that it had begun to fall before the water pressure maximum was attained. The key problem is why the peak of sliding at the ice–bed interface occurs during water pressure build-up and not at its maximum. Bahr & Rundle (1996) have suggested a statistical stick-slip mechanism involving interactions between different basal zones with different stiffnesses, but it can only apply if the relations shown in figure 12 are local and not general.

Iverson *et al.* (1995) found beneath Storglaciären in Sweden that, although glacier velocity peaks were coeval with effective pressure minima, they coincided with minimum, often negative strain rates in the underlying till measured by tilt meters in the till. They suggested that effective pressure minima produced enhanced sliding at the ice–bed interface, but produced little shear strain in the till as a consequence of decoupling between the ice and till. This permitted vertical expansion to take place in the unloaded till as a consequence of hydraulic pumping. This, together with the calculation by Iverson *et al.* (1995) that the till could only bear a relatively small part of the basal shear stress suggests that the till lay in hollows in bedrock, and that it could therefore be unloaded, permitting water pressure inflation of the till in the inter-ridge troughs. The absence of rock ridges penetrating through the till at Breidamerkurjökull appears to preclude such a mechanism there.

(d) *Disparities between trends in displacement rates between* $T_{0.1}$ *and* $T_{0.5}$.

In some parts of the record there are several sustained periods during which the velocity of $T_{0.5}$ decreases and then increases with respect to the velocity of $T_{0.1}$, to an extent greater than that expected from the strain profile (figure 13), and associated with an increase and then decrease in the water pressure measured at $T_{0.5}$. We suggest that this reflects movement of the deforming mass over an obstacle (probably a deeply embedded boulder) on the surface of decollement between the deforming and stable horizons. We expect the relative velocity between adjacent strain markers to increase and decrease in an approximately symmetrical way as shear strains increase and decrease as till deforms over and around the boulder. However, we expect undrained loading of the till as it moves towards the boulder to produce a relatively high water pressure on the up-glacier side of the boulder, and relatively low pressure as the till swells in the lee of the boulder. The pattern of hysteresis is very similar to that noted by Boulton *et al.* (1979) in the stresses measured at a point on a glacier bed as boulders embedded in basal ice passed over it.

(e) *Vertical trends of water pressure and effective pressure can be reversed during diurnal water pressure cycles.*

Figure 14*a* shows water pressure fluctuations as measured by the transducers in the till during a 24 h period from 00.00 on day 258 to 00.00 h on day 259.

Downloaded from rsta.royalsocietypublishing.org

There is a downward water pressure gradient in the till at 00.00, which we suggest reflects flow of water derived from basal melting towards the underlying lower pressure aquifer. Aquifer pressures continue to decline until after 06.00, but rise strongly later during the morning, so that by 12.00, water pressure in the aquifer has risen above the pressure at the top of the till producing water injection into the till from below. Indeed, between 06.00 and 12.00, there is a transient water pressure profile reflecting simultaneous injection both from top and bottom. As the rate of water pressure rise in the aquifer diminishes, flow from recharge at the glacier sole causes a reversal of the water pressure gradient by 18.00. Subsequently, water pressure in the aquifer falls by 00.00 h on day 259 to just above the water pressure at the beginning of the day. The changes in inferred effective pressure generated through this diurnal cycle are shown in figure 14*b*. It shows that during the middle of the day, effective pressures were lower at the base of the till than at the top. We might therefore expect strain rates at the base of the till to be larger than those at higher levels. Unfortunately, the displacement record is not of sufficient resolution on day 258 to verify this, although neither does it deny it. Such variations in the horizon of maximum shear strain have important implications for the hydraulic interpretation of glacier tectonic structures. Although the reversal in the effective pressure gradient was a rare event during the experiment, there are settings where it could be the norm.

The local component of shear stress computed from ice thickness and slope was nearly constant during the experiment, although we were not able to estimate the longitudinal stress component. An estimate of relationships between strain rate and effective pressure, assuming constant shear stress, suggested a power law fit of $\dot{\varepsilon} = 2.73 \times 10^5 p_e^{-2.23}$.

7. Large-scale effects

If, as we suggest, the spatial organization and efficiency of drainage beneath glaciers plays a major role in determining the large-scale deformational behaviour of tills, then laboratory and small-scale field experiments alone are not an adequate basis from which to deduce their large-scale behaviour. Figure 3 shows the general erosional and depositional consequences of different assumptions about the large-scale rheological behaviour of tills transported and deposited by the process of subglacial shear deformation.

If the global behaviour of a sediment is of class A (large n, figure 2), glacial erosion rates over it will tend to be low and the tills produced from it by deformation will tend to be thin. Sediments of class B, which show significant strain hardening or viscous behaviour (low n), will tend to suffer high glacial erosion rates and produce thick tills. Thus, where we can be sure that a till has been transported by shear deformation, we should be able qualitatively to assess its large-scale rheological behaviour during transport. Such an example of this has been presented by Boulton *et al.* (1996). Archives and modern observations permitted a detailed reconstruction of the rapid surge of the glacier Sefströmbreen in Spitsbergen, which produced an advance of 6 km in a period of less than 14 years across an arm of the sea and onto an island. There is strong evidence that sea-bottom muds were transported by shearing beneath the glacier and smeared onto the island where they are now exposed for observation

Downloaded from rsta.royalsocietypublishing.org

after glacier retreat, showing fold structures which reflect shear deformation (cf. figure 9). The minimum rate of shear transport of sediment onto the island was about 2000 m^2 a^{-1} per metre width of glacier; a rate about 1000× greater than that beneath Breidamerkurjökull (figure 8). It could only have been achieved if shear deformation had occurred to a significant depth below the moving glacier sole, suggesting that the large-scale behaviour of the deforming sediment must have been of class B rather than the very highly nonlinear–perfectly plastic response of class A.

It has been suggested that subglacial shearing of sediment is also the predominant process whereby the thick till sequences of lowland areas of North America and Eurasia were transported and emplaced. If this was so, then its implication would again be that global class B behaviour was common or dominant during ice-sheet glaciation of these areas, and that it applied both to the relatively coarse-grained tills of the ancient shield areas which lay in the centre of glaciation and the fine-grained tills of the surrounding areas (figure 5). However, although there are many localities at which pervasive subglacial deformation of tills has been claimed (e.g. Hart 1995), it has not yet been demonstrated that this is true of the majority of tills in these areas.

8. From continuum descriptions to interparticle mechanisms

We have described or inferred the deformation of tills or analogous sediments in continuum terms which suggest that particulate sediments beneath glaciers can show viscous properties. This has important implications for the nature of coupling between a glacier and its bed, for processes and magnitudes of glacial erosion and deposition and for the evolution of geotechnical properties in tills. What are the mechanisms at the particulate level which determine this behaviour?

In clay soils, there is evidence of a strongly nonlinear dependency of strain rate on shear stress. The particle level mechanisms which lead to this behaviour are potentially complex compared to those of sands because of the complexity of clay microstructure. Individual clay mineral plates are often parts of electrically bound flocs, much of the water is electrically trapped within the structure and water chemistry plays a considerable role in determining physical properties. On the application of stress, we expect elastic deformation of flexible clay particles or clusters and permanent, plastic deformation due to the breaking of interparticle bonds (particularly in flocculated clays). We expect sustained viscous deformation, as a nonlinearly viscous fluid (e.g. Rosenqvist 1963), to occur as clay particles, separated by interstitial water, move with respect to each other in response to stress. This is likely to occur most readily if clay particles are not part of large complex clusters. Thus, sustained deformation which breaks down the floc structure of a clay may progressively reduce its viscosity.

We expect a clay without a significant clast fraction to show the extreme nonlinearity suggested by Kamb (1991). However, tills are typically mixed-grain deposits (figure 5) and even the most clay rich tills show significant clast proportions (coarse silt, sand, gravel). In a dominantly clay sediment undergoing distributed shear strain, but which contains some clasts ‘floating’ in the clay matrix, we would expect larger clasts which ‘bridge’ across a clay zone undergoing shear, to divert flow of clay around it, and thus reduce the effective viscosity of the clay. Where clasts are close together, the associated patterns of divergence and convergence may interact, pro-

Downloaded from rsta.royalsocietypublishing.org

ducing a quasi-granular effect. We suggest that the Lowestoft Till (figure 5) may be in the this category of strain blocking. If shear is highly localized along relatively well-defined planes, clasts intersecting the planes may produce kinematic blocking of shear or at least cause ploughing along the plane.

Where concentrations of sand or coarser clasts exceed 30–40%, relatively long-range chains of particles in contact tend to develop. These begin to carry a significant proportion of the force transmitted through the sediment (Drescher & de Joselin de Jong 1972; Adams 1996), and because of mobilization of friction and particle interlocking to contribute a significant proportion of the resistance to deformation. Shear strain of the assemblage will, however, continually disrupt the chains so that hitherto unloaded particles become parts of newly reorganized force transmission pathways (Thornton 1996). Where clasts are large and frequent, both interlocking and friction will ensure that strain in an immediately subglacial sediment will be transmitted to depth. Moreover, much deformation in the matrix will tend to be kinematically blocked by clusters and chains of frictionally interacting or interlocking particles. We expect such mixed grain sediments (such as the Drenthe Till and the Magnus Clay) to exhibit rate dependence derived from its matrix, but with a diminished nonlinearity as a consequence of relatively high clast frequencies.

It has been usual to contrast rate dependence in cohesive, clay rich sediments with rate independence in frictional, sandy sediments (e.g. Dafalias 1984). The evidence of rate dependence in many poorly sorted sediments with a predominantly sandy matrix, including tills, is surprising. Skinner (1969) showed that the coefficient of static friction for a relatively dense granular assemblage was independent of intergranular friction, suggesting that particle interlocking provided the dominant resistance to failure. The stress required to produce failure is that which causes the assemblage to dilate sufficiently to produce 'unlocking' of the structure and for trains of grains to move freely in sustained flow over each other (cf. Drake 1990). This elasto-plastic response is associated with a fall in stress to a residual level associated with intergranular friction, and is presumed to occur with a dilated structure and a voids ratio appropriate to the critical state. In an approximately equigranular mass, interconnected, load bearing particle chains are continually being disrupted and reformed. Sliding contacts, which provide the energy dissipative part of the system, will tend to occur in the relatively unloaded areas, and have been shown by simulations (Thornton & Sun 1993) to be reduced in frequency by increased interparticle friction. Increased strain rate will decrease the coordination number and increase the frequency of non-load bearing particles.

In a mixed grain, sandy sediment, such as a sandy till, we expect a relatively high frequency of outsize clasts or clusters of clasts. Such an interlocked cluster in a zone of shear will tend to block deformation and cause a local stress build up, until the disruption of the stress field causes readjustment of grain packing or stress builds up sufficiently to cause grain fracture, so that local unlocking takes place and local deformation resumes. These are the conditions under which a stick-slip regime develops (Rabinowicz 1958). In friction between solids, rate dependence occurs because of increase of friction during stick events as the log of time, and decrease during slip events as the log of slip velocity. In a deforming granular mass with outsize clasts, the frequency of blocking (stick) events will depend upon the rate of strain, which will therefore show stress dependence. Shear tests of sandy tills which remove the coarse fraction may therefore seriously underestimate this property. The

PHILOSOPHICAL TRANSACTIONS OF THE ROYAL SOCIETY A MATHEMATICAL, PHYSICAL & ENGINEERING SCIENCES

PHILOSOPHICAL TRANSACTIONS OF THE ROYAL SOCIETY A MATHEMATICAL, PHYSICAL & ENGINEERING SCIENCES

Downloaded from rsta.royalsocietypublishing.org

importance of grain fracture in a deforming sandy till has been well demonstrated (Boulton *et al*. 1974; Hiemstra & van der Meer 1997).

We suggest that the immediate opportunities for understanding the particle interactions which determine the observed behaviour of these systems lie in computer simulations of the behaviour of discrete particle assemblages coupled with appropriate experimentation. This should lead to a better physical formulation of rheological rules for the range of variation of natural materials and analysis of their behaviour in realistic approximations of their setting.

For their assistance and advice in the laboratory and in the field we thank Richard Hindmarsh, Nick Hulton, Sergei Zatsepin, Flosi and Sigurdur Bjornsson, Fred Eybergen, Nick Hulton, Mike Paul, Hugh Barras, David Ponniah and Floris Schokking. Trevor Poskitt and David Muir Wood also made helpful comments. Much of the work was supported by research grants from NERC (GR3/5253 and GR3/9220) the European Commission (F12W/0046) and the Royal Society.

References

Adams, M. J. 1996 The uniaxial compaction of particle assemblies. In *Solid interactions* (ed. M. J. Adams, S. K. Biswas & B. K. Briscoe), pp. 265–280. London: Imperial College Press.

Alley, R. B. 1991 Deforming-bed origin for southern Laurentide till sheets? *J. Glaciology* **37**, 67–76.

Alley, R. B., Blankenship, D. D., Bentley, C. R. & Rooney, S. T. 1986 Deformation of till beneath ice stream B, West Antarctica. *Nature* **322**, 57–59.

Bagnold, R. A. 1954 Experiments on a gravity-free dispersion of large solid spheres in a Newtonian fluid under shear. *Proc. R. Soc. Lond.* A **225**, 49–63.

Bahr, D. B & Rundle, J. B. 1996 Stick-slip mechanics at the bed of a glacier. *Geophys. Res. Lett.* **23**, 2073–2076.

Barden, L. 1965 Consolidation of clay with non-linear viscosity. *Géotechnique* **15**, 345–362.

Bishop, A. W., Green, G. E., Garga, V. K., Andersen, A. & Brown, J. D. 1971 A new ring shear apparatus and its application to the measurement of residual strength. *Géotechnique* **21**, 273–328.

Blake, E. W. & Clarke, G. K. C. 1992 Interpretation of borehole-inclinometer data: a general theory applied to a new instrument. *J. Glaciology* **38**, 113–124.

Blake, E. W., Clarke, G. K. C. & Gerin, M. C. 1992 Tools for examining subglacial bed deformation. *J. Glaciology* **38**, 388–396.

Blake, E. W., Fischer, U. H. & Clarke, G. K. C. 1994 Direct measurement of sliding at the glacier bed. *J. Glaciology* **40**, 595–599.

Bógadottir, H., Boulton, G. S., Tómasson, H. & Thors, K. 1985 The structure of sediments beneath Breidamerkursandur and the form of the underlying bedrock. In *Iceland Coastal and River Symp.* (ed. G. Sigbjarnarson). Reykjavik, Iceland: National Energy Authority.

Boltzmann, L. 1896 *Vorlesungen über Gastheorie*. Leipzig: Barth. (English transl. S. G. Brush, *Lectures on gas theory*, University of California Press, Berkeley, 1964.)

Boulton, G. S. 1987 A theory of drumlin formation by subglacial sediment deformation. In *Drumlin Symp.* (ed. J. Menzies & J. Rose), pp. 25–80. Rotterdam: Balkema.

Boulton, G. S. 1996 Theory of glacial erosion, transport and deposition as a consequence of subglacial sediment deformation. *J. Glaciology* **42**, 43–62.

Boulton, G. S. & Dobbie, K. E. 1993 Consolidation of sediments by glaciers: relations between sediment geotechnics, soft-bed glacier dynamics and subglacial groundwater flow. *J. Glaciology* **39**, 26–44.

Boulton, G. S. & Hindmarsh, R. C. A. 1987 Sediment deformation beneath glaciers: rheology and geological consequences. *J. Geophys. Res.* B **92**, 9059–9082.

Downloaded from rsta.royalsocietypublishing.org

Boulton, G. S. & Jones, A. S. 1979 Stability of temperate ice caps and ice sheets resting on beds of deformable sediment. *J. Glaciology* **24**, 29–43.

Boulton, G. S., Dent, D. L. & Morris, E. M. 1974 Subglacial shearing and crushing, and the role of water pressures in tills from south-east Iceland. *Geografiska Annlr* A **56**, 135–145.

Boulton, G. S., Morris, E. M. & Armstrong, A. A. 1979 Direct measurement of stress at the base of a glacier. *J. Glaciology* **22**, 3–24.

Boulton, G. S., Van der Meer, J. J. M., Hart, J., Beets, D., Ruegg, G. H. J., Van der Wateren, F. M. & Jarvis, J. 1996 Till and moraine emplacement in a deforming bed surge—an example from a marine environment. *Quaternary Sci. Rev.* **15**, 961–987.

Clarke, G. K. C. 1987 Subglacial till: a physical framework for its properties and processes. *J. Geophys. Res.* **92**, 9023–9036.

Clayton, K. M. 1999 Quantification of the impact of glacial erosion on the British Isles. (In the press.)

Coussot, P. & Piau, J.-M. 1995 The effects of an addition of force-free particles on the rheological properties of fine suspensions. *Can. Geotech. Jl* **32**, 3971–3974.

Dafalias, Y. D. 1984 On rate dependence and anisotropy in soil constitutive modelling. In *Constitutive relations for soils* (ed. G. Gudehus, F. Darve & I. Vardoulakis), pp. 457–462. Rotterdam: Balkema.

Drake, T. G. 1990 Structural features in granular flow. *J. Geophys. Res.* **95**, 8681–8696.

Drescher, A. & de Joselin de Jong, G. 1972 Photoelastic verification of a mechanical model for the flow of a granular material. *J. Mech. Phys. Solids* **20**, 337.

Georgiannou, G., Burland, J. B. & Hight, D. W. 1990 The undrained behaviour of clayey sands in triaxial compression and extension. *Géotechnique* **40**, 431–449.

Glen, J. W. 1955 The creep of polycrystalline ice. *Proc. R. Soc. Lond.* A **228**, 519–538.

Hart, J. K. 1995 Subglacial erosion, deposition and deformation associated with deformable beds. *Prog. Phys. Geography* **19**, 173–191.

Hart, J. K. & Boulton, G. S. 1991 The interrelation of glaciotectonic and glaciodepositional processes within the glacial environment. *Quaternary Sci. Rev.* **10**, 335–350.

Heerema, E. P. 1979 Relationships between wall friction displacement velocity and horizontal stress in clay and in sand for pile driveability analysis. *Ground Engng.*

Hiemstra, J. F. & van der Meer, J. J. M. 1997 Pore-water controlled grain fracturing as an indicator for subglacial shearing in tills. *J. Glaciology* **43**, 446–454.

Humphrey, N., Kamb, B., Fahnestock, M. & Engelhardt, H. 1993 Characteristics of the bed of the Lower Columbia glacier. *J. Geophys. Res.* **98**, 837–846.

Iverson, R. M. 1985 A constitutive equation for mass-movement behaviour. *J. Geology* **93**, 143–160.

Iverson, R. M. 1997 The physics of debris flows. *Rev. Geophys.* **35**, 245–296.

Iverson, N. R., Hanson, B., Hooke, R. LeB. & Jansson, P. 1995 Flow mechanism of glacier soft beds. *Science* **267**, 80–81.

Jenson, J. W., MacAyeal, D. R., Clarke, P. U., Ho, C. L. & Vela, J. C. 1996 Numerical modelling of subglacial sediment deformation: implications for the behaviour of the Lake Michigan Lobe, Laurentide ice sheet. *J. Geophys. Res.* **101**, 8717–8728.

Johnson, P. C. & Jackson, R. 1987 Frictional-collisional constitutive relations for granular materials, with application to plane shearing. *J. Fluid Mech.* **176**, 67–93.

Kamb, B. 1991 Rheological nonlinearity and flow instability in the deforming bed mechanism of ice stream motion. *J. Geophys. Res.* **96**, 16 585–16 595.

Kumar, G. V. & Muir Wood, D. 1997 Mechanical behaviour of mixtures of kaolin and coarse sand. In *Mechanics of granular and porous materials* (ed. N. A. Fleck & A. C. F. Cocks), pp. 57–68. Dordrecht: Kluwer.

Litkouhi, S. & Poskitt, T. J. 1980 Damping constants for pile driveability calculations. *Géotechnique* **30**, 77–86.

PHILOSOPHICAL TRANSACTIONS OF THE ROYAL SOCIETY A MATHEMATICAL, PHYSICAL & ENGINEERING SCIENCES

PHILOSOPHICAL TRANSACTIONS OF THE ROYAL SOCIETY A MATHEMATICAL, PHYSICAL & ENGINEERING SCIENCES

Downloaded from rsta.royalsocietypublishing.org

Lupini, J. F. 1981 The residual strength of soils. PhD thesis, University of London.

Lupini, J. F., Skinner, A. E. & Vaughan, P. R. 1981 The drained cohesive strength of cohesive soils. *Géotechnique* **31**, 181–213.

MacAyeal, D. R. 1992 Irregular oscillations of the West Antarctic ice sheet. *Nature* **359**, 29–32.

Maxwell, J. C. 1866 On the dynamical theory of gases. *Phil. Trans. R. Soc. Lond.* **157**, 49–88.

Nye, J. F. 1952 The mechanics of glacier flow. *J. Glaciology* **2**, 82–93.

Nye, J. F. 1957 The distribution of stress and velocity in glaciers and ice sheets. *Proc. R. Soc. Lond.* A **239**, 113–133.

O'Brien, J. S. & Julian, P. Y. 1988 Laboratory analysis of mudflow properties. *J. Hydraulic Engng* **114**, 877–887.

Patterson, W. S. B. 1981 *The physics of glaciers*, 2nd edn (380pp). Oxford: Pergamon Press.

Patterson, W. S. B. 1994 *The physics of glaciers*, 3nd edn (480pp). Oxford: Elsevier.

Paul, M. A. & Evans, H. 1974 Observations on the internal structure and origin of some flutes in glaciofluvial sediments, Blomstrandbreen, north-west Spitsbergen. *J. Glaciology* **13**, 393–400.

Phillips, C. J. & Davies, T. R. H. 1991 Determining rheological parameters of debris flow material. *Geomorphology* **4**, 101–110.

Rabinowicz, E. 1958 The intrinsic variables affecting the stick-slip process. *Proc. R. Soc. Lond.* A **71**, 668–675.

Roscoe, K. H. 1970 The influence of strains in soil mechanics. *Géotechnique* **20**, 129–170.

Rosenqvist, I. T. 1963 The influence of physico-chemical factors upon the mechanical properties of clays. Norwegian Geotechnical Institute, Publ. no. 54.

Savage, S. B. & Cheloborad, A. F. 1982 A model for creeping flow in landslides. *Ass. English Geologists Bull.* **19**, 333–338.

Savage, S. B. & Sayed, M. 1984 Stresses developed by dry cohesionless granular materials sheared in an annular shear cell. *J. Fluid Mech.* **142**, 391–430.

Schmid, W. E., Klausner, Y. & Whitmore, C. F. 1960 Rheological shear and consolidation behaviour of clay soils. Progress Report to Office of Naval Research, Department of the Navy, Washington, DC.

Skinner, A. E. 1969 A note on the influence of interparticle friction on the shearing strength of a random assemblage of spherical particles. *Géotechnique* **19**, 150–157.

Swanston, D. N., Ziemer, R. R. & Janda, R. J. 1983 Influence of climate on progressive hillslope in Redwood Creek valley, northwest California. US Geological Survey Open-file Report, 83–259, 42pp.

Taylor, D. W. 1942 Research on consolidation of clays. Massachusetts Institute of Technology, Department of Civil and Sanitary Engineering, Serial 82.

Taylor, D. W. & Merchant, W. 1940 A theory of clay consolidation accounting for secondary compression. *J. Math. Phys.* **19**, 167–185.

Terzaghi, K. 1925 *Erdbaumechanik*. Vienna: Franz Deuticke.

Terzaghi, K. 1941 Undisturbed clay samples and undisturbed clays. *J. Boston Soc. Civil Engrs* **28**(3), 211–231.

Thornton, C. 1996 From contact mechanics to particulate mechanics. In *Solid–solid interactions* (ed. M. J. Adams, S. K. Biswas & B. J. Briscoe), pp. 250–264. London: Imperial College Press.

Thornton, C. & Sun, G. 1993 Axisymmetric compression of 3D polydisperse systems of spheres. In *Powders and grains* (ed. C. Thornton). Rotterdam: Balkema.

Trenter, N. A., Wilson, S. L. S. & Stewart, F. S. 1997 Engineering in glacial tills. Construction Industry Research and Information Association, Research Project RP 514, 256pp.

Wilkinson, W. L. 1960 *Non-Newtonian fluids—fluid mechanics, mixing and heat transfer* (130pp). New York: Pergamon Press.

PHILOSOPHICAL TRANSACTIONS OF THE ROYAL SOCIETY A MATHEMATICAL, PHYSICAL & ENGINEERING SCIENCES

PHILOSOPHICAL TRANSACTIONS OF THE ROYAL SOCIETY A MATHEMATICAL, PHYSICAL & ENGINEERING SCIENCES

Downloaded from rsta.royalsocietypublishing.org

Winter, M. G., Holmgeirsdöttir, Th. & Suhardi, J. 1998 The effect of large particles on acceptability determination for earthworks compaction. *Q. Jl Engng Geol.*

Wladis, D., Jonsson, P. & Wallroth, T. 1997 Regional characterization of hydraulic properties of rock using well test data. Svensk Karnbranslehantering AB, Technical Report, 97–29, 40pp.

Wong, W. W. H., Ho, C. L., Iverson, R. M. & Hovind, C. L. 1995 Evaluation of viscoplastic slope movement based on triaxial tests. In *Clay and shale slope instability* (ed. W. C. Haneberg & S. A. Anderson). *Geological Soc. Am. Rev. Engng Geol.* **10**, 39–50.

PHILOSOPHICAL TRANSACTIONS OF THE ROYAL SOCIETY A MATHEMATICAL, PHYSICAL & ENGINEERING SCIENCES

PHILOSOPHICAL TRANSACTIONS OF THE ROYAL SOCIETY A MATHEMATICAL, PHYSICAL & ENGINEERING SCIENCES

Downloaded from rsta.royalsocietypublishing.org

PHILOSOPHICAL TRANSACTIONS OF THE ROYAL SOCIETY A MATHEMATICAL, PHYSICAL & ENGINEERING SCIENCES

PHILOSOPHICAL TRANSACTIONS OF THE ROYAL SOCIETY A MATHEMATICAL, PHYSICAL & ENGINEERING SCIENCES